DOKUZ EYLÜL UNIVERSITY
GRADUATE SCHOOL OF NATURAL AND APPLIED SCIENCES

MELTING OF A PHASE CHANGE MATERIAL ON A FINNED-TUBE HEAT EXCHANGER

by
Kamber Naci ÜSTÜNER

September, 2007
İZMİR

MELTING OF A PHASE CHANGE MATERIAL ON A FINNED-TUBE HEAT EXCHANGER

A Thesis Submitted to the
Graduate School of Natural and Applied Sciences of Dokuz Eylül University
In Partial Fulfillment of the Requirements for the Degree of Master of Science
in Mechanical Engineering, Thermodynamics Program

by

Kamber Naci ÜSTÜNER

Sebtember, 2007
İZMİR

M.Sc THESIS EXAMINATION RESULT FORM

We have read the thesis entitled **"MELTING OF A PHASE CHANGE MATERIAL ON A FINNED-TUBE HEAT EXCHANGER"** completed by **KAMBER NACİ ÜSTÜNER** under supervision of **ASST. PROF. TAHSİN BAŞARAN** and we certify that in our opinion it is fully adequate, in scope and in quality, as a thesis for the degree of Master of Science.

Asst. Prof. Tahsin BAŞARAN

Supervisor

(Jury Member)

(Jury Member)

Prof.Dr. Cahit HELVACI
Director
Graduate School of Natural and Applied Sciences

ACKNOWLEDGMENTS

I would like to thank to my advisors Asst. Prof. Tahsin Başaran and Prof. Dr. Nuri Kayansayan for their guidance.

I would also like to thank Tech. Alim Zorluol for providing his expertise.

Kamber Naci ÜSTÜNER

MELTING OF A PHASE CHANGE MATERIAL ON A FINNED-TUBE HEAT EXCHANGER

ABSTRACT

In this thesis study, an experimental investigetion is carried out for solidification and melting of a phase change material around a horizontal finned tube. The effects of some geometrical and flow parameters on charging and discharging of the cold thermal energy are investigated. Afterwards the experiment results are compared with each other. The aim of this study is to reveal the changes in the amount of stored thermal energy by changing the fin diameter, fin spacing and the flow rate of the heat transfer fluid. It is shown that each of the parameters affects the amount of stored or released cold thermal energy in a different rate.

Keywords: Thermal energy storage, Melting, Finned tube, Phase change material

KANATLI BORU TİPİ BİR ISI EŞANJÖRÜNÜN ÜZERİNDEKİ BİR FAZ DEĞİŞİM MALZEMESİNİN ERİMESİ

ÖZ

Bu tez çalışmasında yatay bir kanatlı boru etrafındaki faz değişim malzemesinin katılaşması ve erimesi için deneysel bir inceleme gerçekleştirilmiştir. Bazı geometrik ve akış parametrelerinin soğu enerjisinin depolanması ve açığa çıkması üzerindeki etkileri incelenmiştir. Daha sonra deney sonuçları birbirleri ile karşılaştırılmıştır. Bu çalışmanın amacı, kanat çapı, kanat aralığı ve ısı transfer akışkanının debisini değiştirerek depolanan ısıl enerji miktarındaki değişimleri ortaya çıkartmaktır. Her bir parametrenin depolanan ya da açığa çıkarılan soğu enerji miktarını değişik bir oranda etkilediği gösterilmiştir.

Anahtar sözcükler: Isıl enerji depolama, Erime, Kanatlı boru, Faz değişim malzemesi

CONTENTS

Page

CHAPTER ONE
INTRODUCTION

1.1 Thermal Energy Storage

Energy storage is the storing of some form of energy that can be drawn upon at a later time to perform some useful operation. Thermal energy storage can refer to a number of technologies that store energy in a thermal reservoir for later reuse. They can be employed to balance energy demand between day time and night time. The thermal reservoir may be maintained at a temperature above (hotter) or below (colder) than that of the ambient environment.

1.1.1 Cold Thermal Energy Storage

The principal application today is the production of ice, chilled water, or eutectic solution at night, which is then used to cool environments during the day. Today, thermal energy storage systems are very popular in the world, especially in the United States and Europe countaries. It is because of the fact that these systems are the most efficient methods to avoid costly energy price and to reduce summer time peak load electricity demand. Cooling demand increases in the hot summer days. Because of this increase, electrical power demand also reaches its peak levels. Thermal energy storage systems convert cooling energy to use at non peak times. They also reduce energy consumption, depending on site-specific design, notably where chillers can be operated at full load during the night (Ermiş, Erek, & Dinçer, 2007).

High peak summertime loads drive the capital expenditures of the electricity generation industry. The industry meets these peak loads with low-efficiency peaking power plants, usually gas turbines, which have lower capital costs but higher fuel costs. A kilowatt-hour of electricity consumed at night can be produced at much lower marginal cost. Utilities have begun to pass these lower costs to consumers.

The solid-liquid phase change is one of the techniques for storing cold thermal energy. This technique has caused a particular reaction in the energy storage area lately. A large part of the base load can be used by using this technique. For this reason, the maximum generating capacity of a cooling equipment can be decreased (ASHRAE, 1987).

1.1.2 Energy Storage with PCM

The latent thermal energy storage using a phase change material (PCM) has attracted attention in the energy storage area extensively. Because during the solidification and melting processes, PCMs have benefits of high energy storage density and isothermal operating characteristics such as charging and discharging heat at a nearly constant temperature. These advantages are good for efficient operation of thermal systems. In recent years, the usage of the latent heat of a PCM as a thermal energy storage substance has interested areas like refrigeration and air conditioning systems, solar energy systems, space craft, heating and cooling of buildings etc. Nevertheless, practical difficulties may occur in applying the latent heat method occasionally. Low thermal conductivity of the PCM, density change, stability of properties under extended cycling and sometimes phase segregation and subcooling of the PCMs are some reasons of these difficulties (Akgün, Aydın, & Kaygusuz, 2006).

The solidification or melting periods of a particular PCM must be known in order to design a latent heat storage unit. The operating circumstances and the storage configurations also must be known in order to forecast the heat transfer coefficients during the process of phase change. It is seen that two kinds of storage configurations were stuided in the literature. One of them is the shell and tube type heat exchanger. In this kind of heat storage unit, the PCM is put in the shell and the heat transfer fluid flows in the tubes. Ismail and Alves (1986), Cao and Faghri (1991a), Bellecci and Conti (1993), Lacroix (1993) and Zhang and Faghri (1996a) made studies about this configurations. The second configuration is a rigid capsule. The PCM is put in this capsule and the heat transfer fluid flows in a tube which surrounds the capsule. The

shell and tube type heat exchanger is considered as the most hopeful configuration as a latent heat storage system. It provides high efficiency for a minimum volume (Erek, İlken, & Acar, 2005).

Ismail and Alves (1986) made a theoretical model of the shell and tube type heat exchanger for storing energy. A similar problem is also modelled by Cao and Faghri (1991b, 1992). In this model, the heat charging and the recovery processes were carried out by the circulating fluid. The shell wall of the storage unit was presumed to be adiabatic for both of these models. The model of the energy storage in a shell and tube type heat exchanger was also examined by Bellecci and Conti (1993). They used the enthalpy model to solve the problem. Cao and Faghri (1991a) searched the latent heat energy storage systems for annular and countercurrent flows seperately. They stated that the storage system with the countercurrent flow is an efficient method to absorb heat energy (Erek, İlken, & Acar, 2005).

Increasing the heat transfer surface area by using finned surfaces is one of the techniques used in order to increase the amount of energy storage. A great number of researches both experimental and theoretical were done in order to explore the effect of fins with rectangular cross section on the rate of melting and solidification. A study of the solidification around a horizontal finned tube with four different fin spacings was done by Bathelt and Viskanta (1981). Sparrow, Larson and Ramsey (1981) experimentally researched the forms of the frozen layer on finned tubes. In these experiments the finned tube were situated vertically. Padmanabhan and Khrishna (1989) theoretically examined the solidification within two concentric cylinders. The cylinders had longitudinal fins. In that study, a relation regarding the percent of solidification to the fin thickness and length, the number of fins, the Stefan and Fourier numbers of the problem was represented. Sasaguchi and Sakamoto (1989) theoretically investigated the melting event on the same geometry. The noteworthy effect of the natural convection on melting was stated on this study. Lacroix (1993) represented a theoretical model in order to estimate the transient behaviour of a shell and tube heat exchanger by placing the PCM on the shell side

and heat transfer fluid circulating through the finned tube (Erek, İlken, & Acar, 2005).

The fact that heat transfer in a latent thermal energy storage system can be increased by placing internally finned tubes was showed by Zhang and Faghri (1996b). A numerical model for the solidification of PCM around a radially finned tube with a constant inner wall temperature of tube was indicated by Ismail et al. (2000). Numerical experiments were carried out to research the effects of fin thickness, fin material, the number of the fins, aspect ratio of tube arrangement and the tube wall temperature. Erek (1999) also numerically and experimentally researched the solidification around the finned tube. In this study, fully developed velocity profile of the heat transfer fluid in the tube is considered.

1.2 Aims of the Study

Two dimensional phase change event around a horizontal radially finned tube was researched experimentally in this study. Both solidification and melting processes were performed by using the PCM as water. For each experiment, some parameters were changed and the results were obtained. The effects of the fin diameter, fin density and the flow rate of the heat transfer fluid on the charged and discharged cold thermal energy were observed. The important aim of this study is to compare the results of the experiments and to evaluate how tube shape and the flow rate of the heat transfer fluid effect the latent cold thermal energy storage in the solidification and melting processes.

In second chapter of the thesis experimental setup is described schematically and each unit of the setup is explained in detail by addition of some photographs, figures and tables. In third chapter, experimental and postexperimental procedure like computation of the charged and discharged cold thermal energy is explained. In fourth chapter of the thesis, results of the experiments are demonstrated. As a conclusion, the last chapter represents concluding remarks.

CHAPTER TWO
EXPERIMENTAL SETUP

2.1 Introduction

All experiments on this research were performed on the experimental energy storage unit which is shown schematically in Figure 2.1a and 2.1b. In Figure 2.1b a lateral view of the some part of the setup is shown.

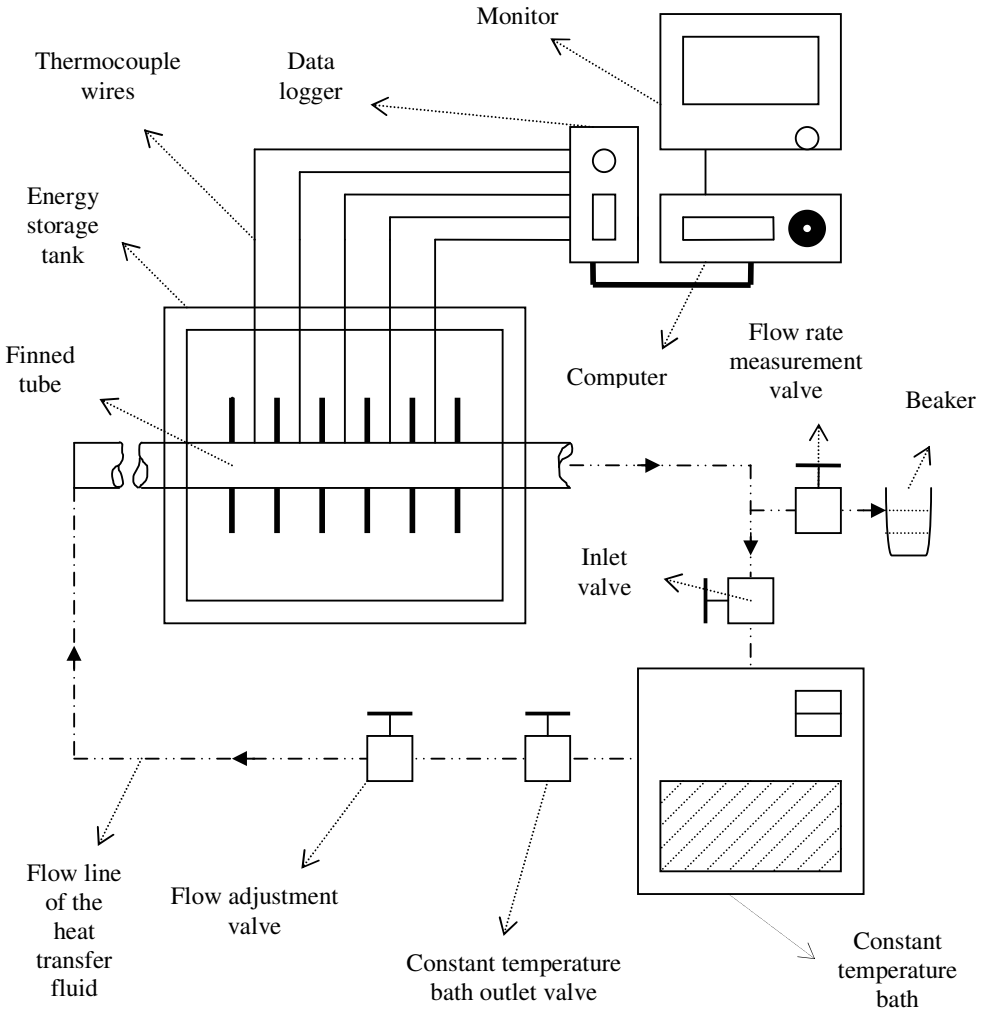

Figure 2.1a Experimental setup

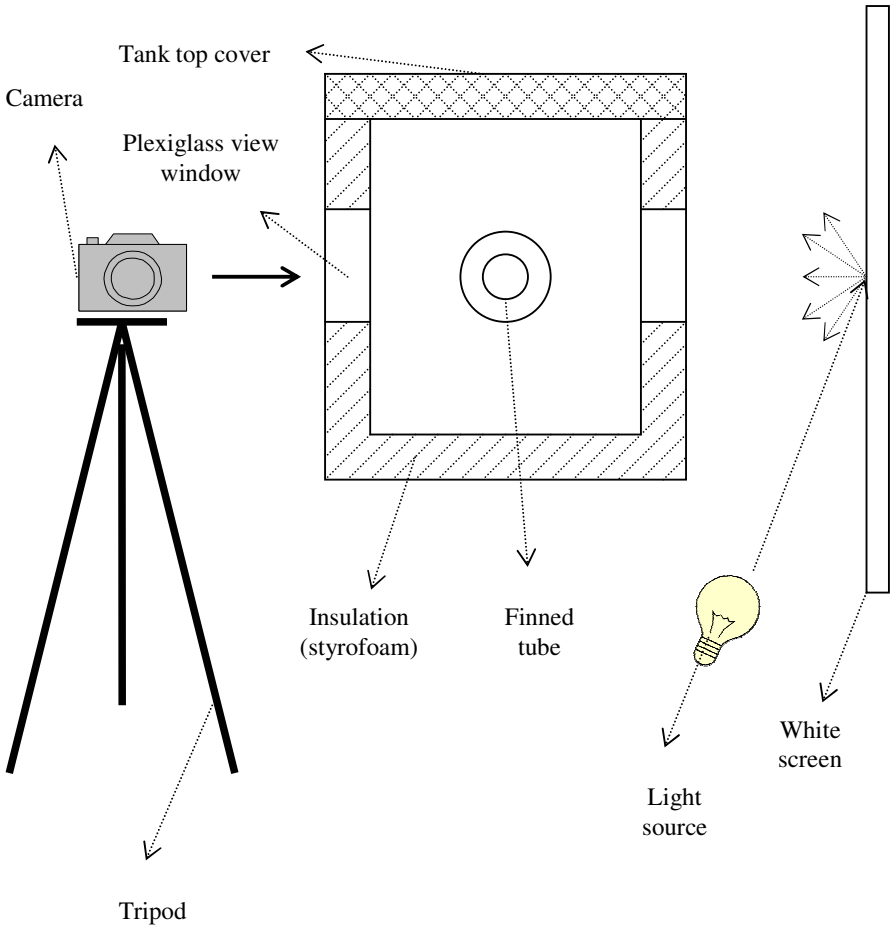

Figure 2.1b Lateral view of the energy storage unit

In Figures 2.2 and 2.3 some photographs of the setup is demonstrated. The photo in Figure 2.2 shows the energy storage tank and thermocouple wires. In Figure 2.3, the flow line of the heat transfer fluid is shown.

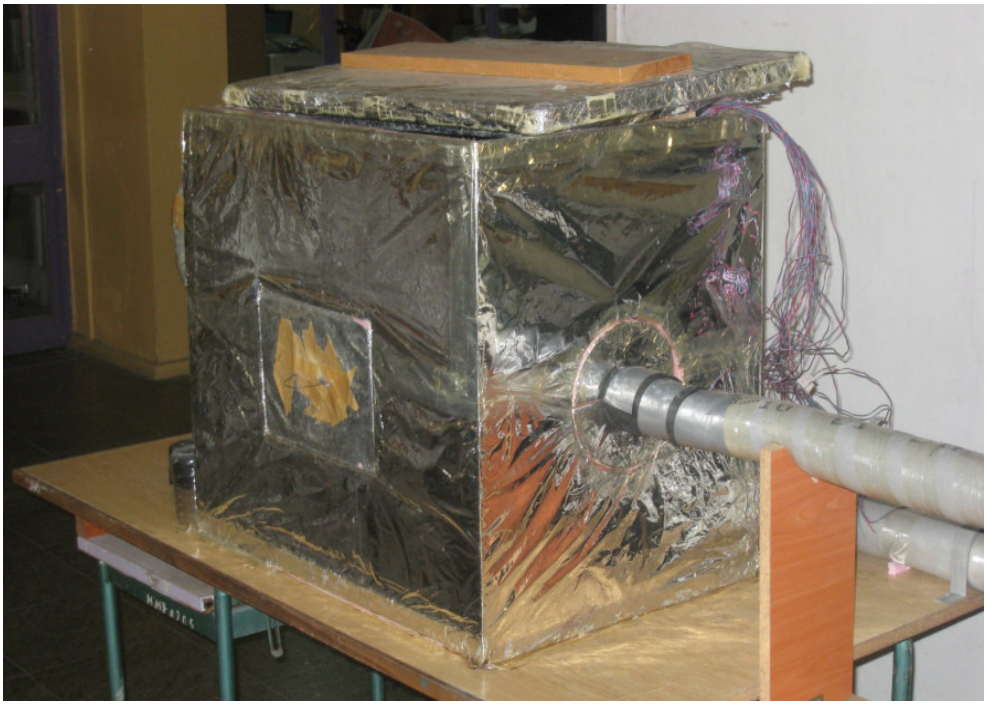

Figure 2.2 Energy storage tank and thermocouple wires

Figure 2.3 The flow line of the heat transfer fluid

Experimental unit mainly consists of these systems:

1. Constant temperature bath
2. The flow system
3. Energy storage unit
4. Temperature measurement system
5. Computer system

These systems are introduced and presented in the following sections of this chapter with all numbered elements of the setup shown in Figure 2.1a and 2.1b.

2.2 Constant Temperature Bath

A Haake brand T model constant temperature bath which is shown in Figure 2.4 was employed to ensure the heat transfer fluid at a certain temperature at the inlet of the test section. This device was appropriate for the experiments. Because the constant temperature bath has the ability of working within a temperature range of -47°C and 100°C with a sensitivity of ±0.1°C and with flow rate of 20 L/min. The storage reservoir of the unit in which the heat transfer fluid was kept has a volume of 30 L. The fluid circulates the whole setup with the aid of a pump inside the device. The constant temperature bath includes a thermostat which keeps the temperature of the heat transfer fluid in the reservoir within the desired range.

Figure 2.4 Constant temperature bath

The flow rate of the heat transfer fluid were controlled by 4 valves. Two valves which are shown in Figure 2.5 were at the entrance and exit of the bath to open or close the circulation of the fluid.

Figure 2.5 The inlet and the outlet valves of the constant temperature bath

The function of the valve which installed after the exit valve of the constant temperature bath was to adjust the flow rate. This valve is demonstrated in Figure 2.6 and also can be seen again in Figure 2.3 that shows the flow pipe line. By adjusting this valve the flow rate was increased or decreased.

Figure 2.6 The flow adjustment valve

The valve which was before the entrance valve of the constant temperature bath as shown in Figure 2.7 was used to measure the flow rate. By opening full this valve and closing the entrance valve, all of the circulating heat transfer fluid were

transferred into a beaker. At an experimental run, the chronometer at zero, the valve directed the fluid to the beaker and after 10 seconds of time elapsed, the valve was switched back to the reservoir position. Then, the content of the beaker was measured and this measured value was multiplied by 6 for one minute flow rate. Thus an average value for the flow rate was estimated.

Figure 2.7 Flow rate measurement valve

The heat transfer fluid was supposed to solidify the phase change material by transferring its cold thermal energy during the solidification processes of the experiments. For this purpose, the temperature of -15°C was tested in the constant temperature bath for solidification. In melting parts of the experiments, temperature was raised to 15°C in order to melt the solidified phase change material. The heat transfer fluid was chosen to be ethyl alcohol (C_2H_5OH) for all experiments in order to provide liquid behaviour at a low temperature such as -15°C. Some thermophysical properties of ethyl alcohol at the temperatures of -15°C and 15°C are shown in Table 2.1. With the flow rate values measured during the experiments, the

values of density and viscosity were used to calculate Reynolds numbers of the heat transfer fluid.

Table 2.1 Thermophysical properties of ethyl alcohol (Chemical Engineering Research Information Center, 2007)

T(°C)	ρ (kg/m^3)	μ (kg/ms)
15	816.4	$1.7x10^{-3}$
-15	842.94	$3.4x10^{-3}$

2.3 The Flow System

As shown in Figure 2.3, the flow section of the experimental setup includes a hydrodynamic entry section. Fully developed flow conditions for the heat transfer fluid at the inlet of the energy storage unit must be provided to ensure the accuracy of the experiment results. Therefore, the hydrodynamic entry section was long enough (240 diameters) to satisfy this necessity at both laminar and turbulent flows of heat transfer fluid (Kays, 1966).

As shown in Figure 2.8, at the return of the flow line and 300 mm away from the exit of the energy storage unit, pipe was raised 150 mm. It was because of the fact that the heat transfer fluid can not fill the piping system completely especially at low Reynolds numbers. So, such an operation was made in order to remove this risk .

The entry length and the return piping sections of the apparatus were made of PVC tubing which had 20 mm inner, 25 mm outer diameter that is shown in Figure 2.9. The advantage of the PVC is that the possibility of pipe corrosion does not exist. The whole length of the flow system including the entry section was approximately 6.5 m. To provide isolation of the flow system, the whole piping was insulated with a 20 mm thick tube covering foam rubber (Acar, 2003).

Figure 2.8 Pipe rise at the exit of the energy storage unit

Figure 2.9 The pipe used for the flow of the HTF

2.4 Energy Storage Unit

The dimensions of the energy storage unit was 450 mm x 550 mm x 600 mm. Energy storage unit also included the finned tube and the phase change material. For the purpose of watching the solidification and melting around the finned tube, the front and the back faces of the storage unit were 10 mm thick plexiglass with 2 mm stainless steel sheet. The other lateral faces were 3 mm thick plexiglass. The bottom surface was also 2 mm thick stainless steel sheet. The bottom surface was covered with 5 cm thick styrofoam layers and the other surfaces (lateral and top surface) were covered with 3 cm thick styrofoam layers for reducing the heat leaks through the surfaces of the unit. A central window with the dimensions of 250 mm x 180 mm which is shown in Figure 2.10 was formed at each styrofoam layer and stainless steel sheet covering the plexiglass surfaces.

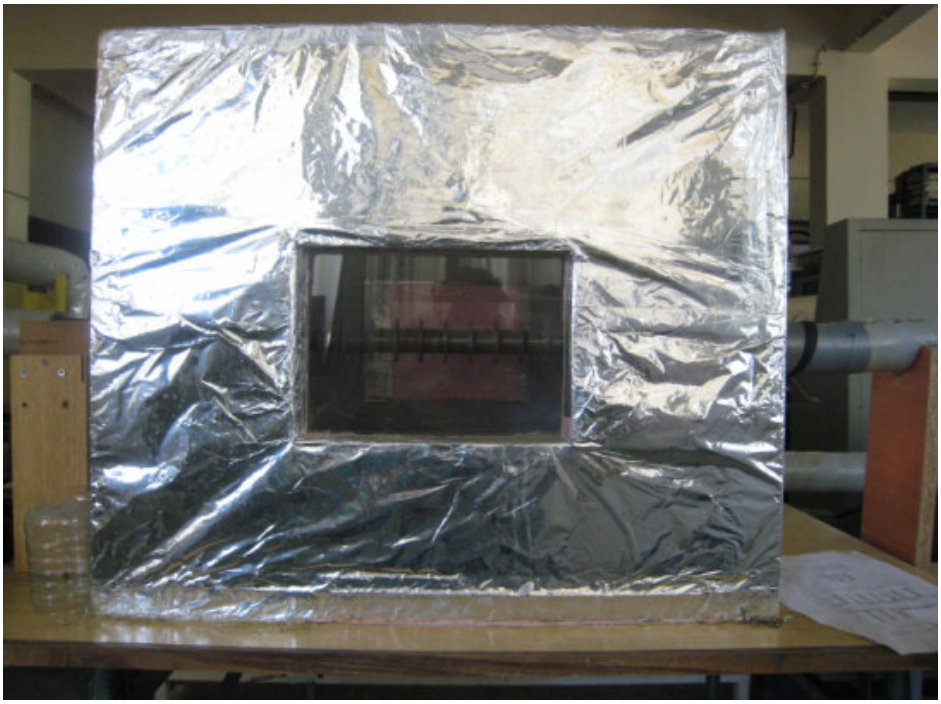

Figure 2.10 Plexiglass view window

Owing to these openings, momentary photographs of solidification and melting of the phase change material could be taken by a digital camera with the help of a light source as shown schematically before in Figure 2.1b. These pictures of solidified and

melted phase change material around the finned tube were transferred from the digital camera to a computer.

As a phase change material, water was selected for the experiments. By removing the 50 mm thick top cover which can be seen back in Figure 2.2, the water could be poured into the storage tank. The thermophysical properties of water is shown in Table 2.2.

Table 2.2 Thermophysical properties of the tube material and PCM (Acar, 2003)

	Tube material	Phase change material	
		Solid	Liquid
ρ (kg/m^3)	8800	916.8	999.8
c_p (J/kg.K)	420	2040	4210
k (W/m.K)	52	2.2	0.567
α (m^2/s)	1.4×10^{-5}	1.35×10^{-7}	
L (J/kg)	-	333500	

In this study, 5 different types of tubes were used in the experiments. Table 2.3 shows the geometrical parameters of all of the tubes tested. As demonstrated in this table, each of the tubes was numbered for an easier expression. In the following sections of this thesis, those numbers are used to define any tube. The finned tubes had circular fins of constant thickness. All of them had the same length of 480 mm and their inner and outer diamaters were 20 mm and 30 mm respectively. But their fin diameters and spacing were different. The parameters for the tubes shown in this table were indicated as a layout in Figure 2.11.

Table 2.3 Geometrical parameters of the tubes used in this study

Tube type	Number of fins	D_i (mm)	D_o (mm)	D_f (mm)	t (mm)	w (mm)
#1	7	20	30	54	3.4	65
#2	7	20	30	64	3.4	65
#3	11	20	30	54	3	40
#4	15	20	30	54	3.5	27.5
#5	Finless tube	20	30	-	-	-

Bronze alloy cylinders were used in the production of the tubes. The chemical content of these solid cylinders was 87.2% Cu, 6.57% Sn, 4.13% Zn, and 1.97% Pb. In Table 2.2, the thermophysical properties of this alloy were given. While producing the tubes, at first the finned surface of the alloy cylinders was an integral piece. Then it was produced by machining on a lathe. At the start of the machining process, the outside diameter of the cylinders was greater than the desired fin diameter. The desired fin and tube sizes were formed at the chip removal process. By producing in this way, the risk of a possible thermal contact resistance between the tube base and the fin was removed (Acar, 2003).

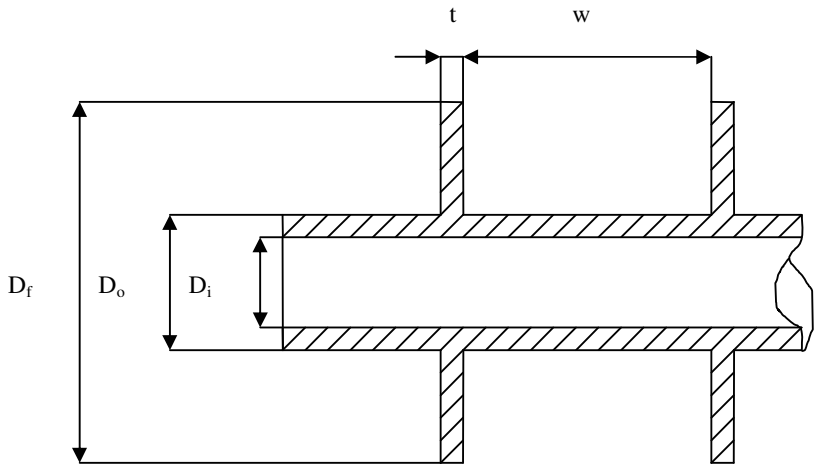

Figure 2.11 Finned tube geometry

The finned tube was situated at the midsection of the energy storage unit and connected to the flow system to fulfill thermally symmetrical conditions in the storage tank. The system was tested for possible leaks after completing the assembly.

The photos of the some of the tubes used in the experiments are shown in Figure 2.12a to 2.12d.

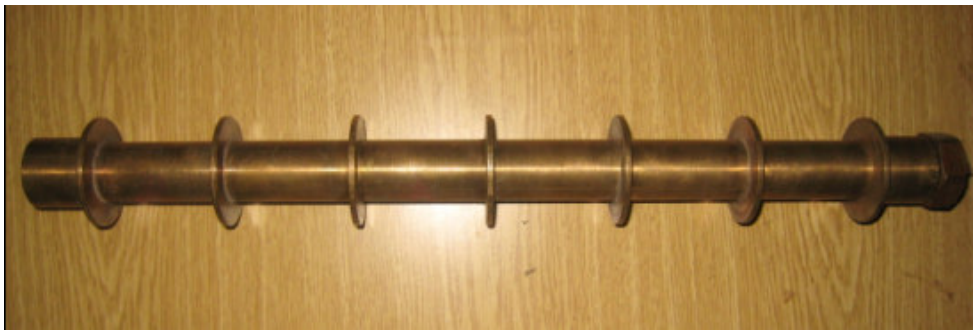

Figure 2.12a The tube #1 (7 finned with small diameter)

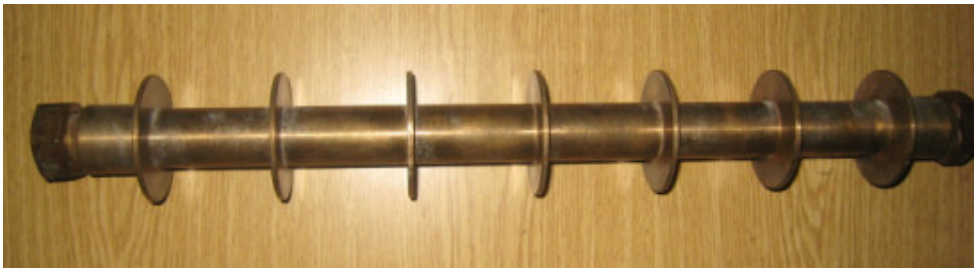

Figure 2.12b The tube #2 (7 finned with big diameter)

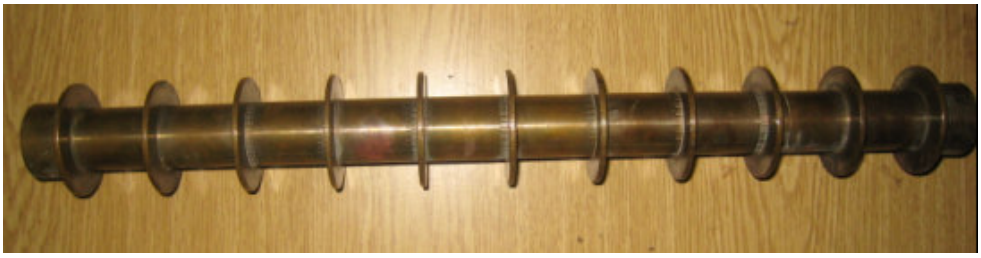

Figure 2.12c The tube #3 (11 finned)

Figure 2.12d The tube #5 (finless)

2.5 Temperature Measurement System

Temperature measurement system consists of thermocouples and data logger. It is essential to measure the temperatures of the finned tube wall and the fin tip for accurate determination of the heat transfer to the phase change material. In this study, type T-24 thermocouples which were manufactured by Omega Engineering Inc. were used as shown in Figure 2.13. Calibration of the thermocouples had been done in the previous experimental studies which were performed a few years ago. It was learned from those studies that 1°C should be added to every measured values in order to get the true temperature values.

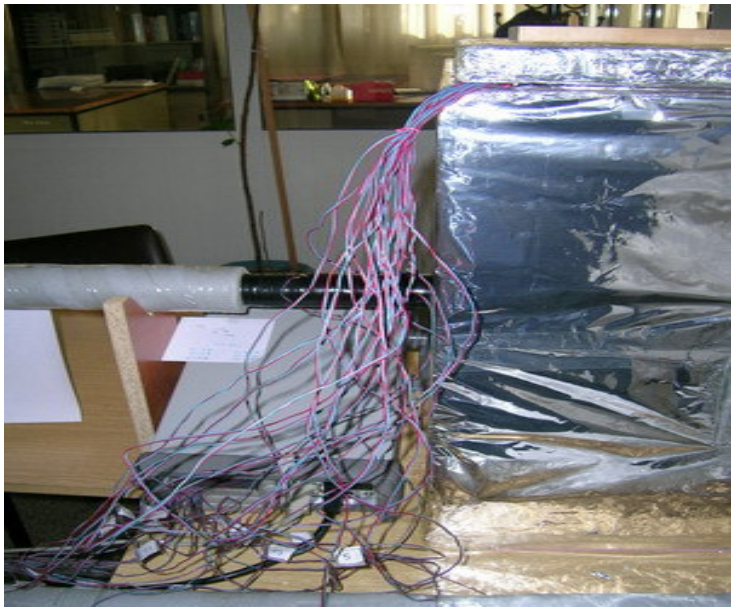

Figure 2.13 Thermocouples used in the experiments

As shown in Figure 2.14, during the experiments, temperatures at 20 different points in the system were measured and recorded. So, for all of the tubes used in the experiments, 20 thermocouples were used. Figure 2.14 demonstrates a model of thermocouple arrangement for the tubes #1 and #2 which have 7 fins. Two thermocouples, which were shown with the numbers of 1 and 2 in that figure, were installed to measure the heat transfer fluid temperatures at the inlet and outlet of the test section.

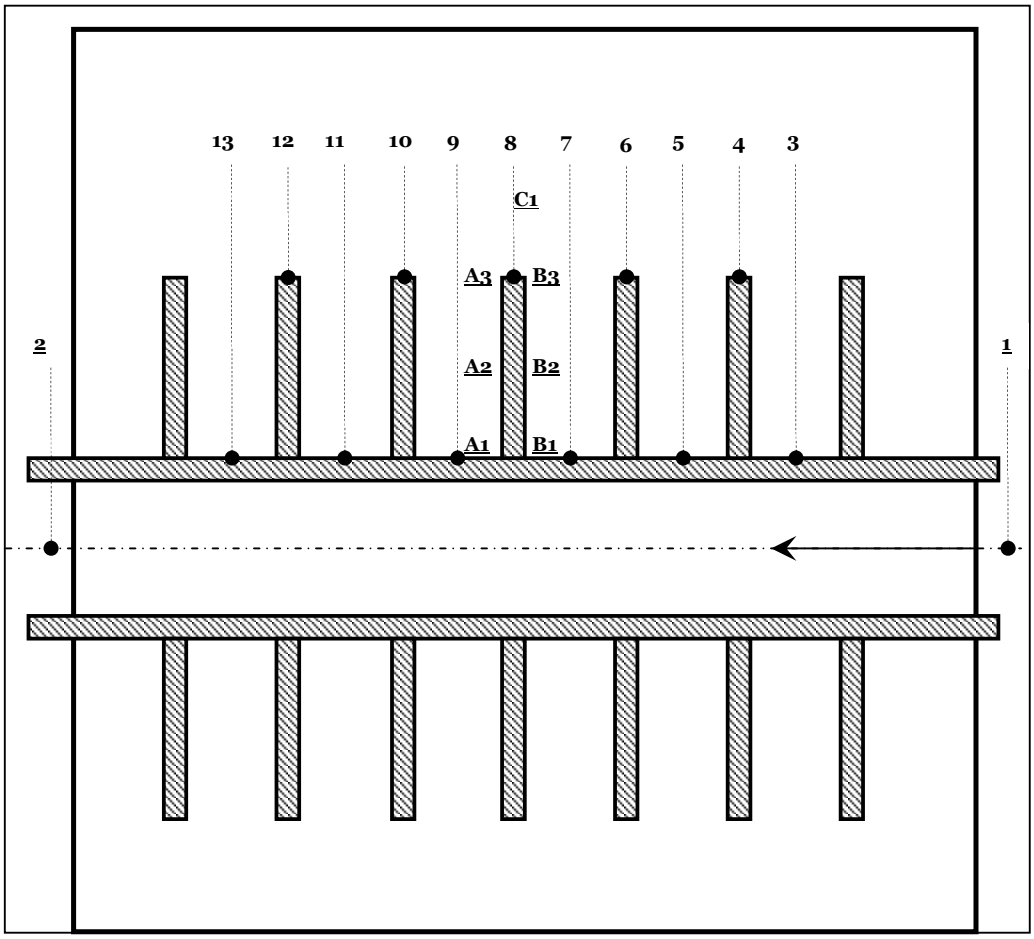

Figure 2.14 Installation of the thermocouples

Because of the large number of temperatures to be measured, the output record of the data was done by the help of a HP type 34970A data logger. With an accuracy of ±1°C, this data logger, which is shown in Figure 2.15, measured the millivolt outputs of the thermocouples. The signal output of the data logger were transmitted and recorded in a personal computer. For this process the software "HP-Benchlink" was used.

The values of temperatures were scanned by the data logger every 30 seconds during both solidification and melting processes. These values could be observed on the computer screen simultaneously by the help of the HP Benchlink software. Also, the inlet and outlet temperatures of the heat transfer fluid could be seen graphically, so the inlet temperature of the alcohol could be kept constant.

Figure 2.15 HP Datalogger

Thermocouple installations for each of the tubes were different. For the tubes #1-2, #3 and #4, this arrangement is shown in Table 2.4a, Table 2.4b and Table 2.4c respectively. For the tube #5, which is the finless tube, the points where the thermocouples installed were the same as the tubes #1 and #2. All thermocouples were installed to the tubes by oxy-acetylene welding.

For the Tables 2.4a to 2.4c, A_1 and B_1 show the left and right base of the middle fin respectively. In accordance with that, A_2 and B_2 show the middle points of the middle fin. A_3 and B_3 show the tip points of the middle fin. The thermocouple number 20 was used for point C_1 which was above and in the line of the middle fin to measure the water temperature. All these points can be seen back in Figure 2.14. The reason of using much more thermocouples near the middle fin is the fact that photographs were taken just ahead of this fin.

Table 2.4a Data logger channel connections for the tubes #1 and #2 (7 fins)

Channel No	**Thermocouple No**	**The point measured**
101	1	Heat transfer fluid inlet temperature
102	2	Heat transfer fluid outlet temperature
103	3	2nd fin base temperature
104	4	2nd fin tip temperature
105	5	3rd fin base temperature
106	6	3rd fin tip temperature
107	7	4th fin base temperature
108	8	4th fin tip temperature
109	9	5th fin base temperature
110	10	5th fin tip temperature
111	11	6th fin base temperature
112	12	6th fin tip temperature
113	13	7th fin base temperature
114	14	A_1
115	15	A_2
116	16	A_3
117	17	B_1
118	21	B_2
119	22	B_3
120	20	C_1

Table 2.4b Data logger channel connections for the tube #3 (11 fins)

Channel No	**Thermocouple No**	**The point measured**
101	1	Heat transfer fluid inlet temperature
102	2	Heat transfer fluid outlet temperature
103	3	3rd fin base temperature
104	4	3rd fin tip temperature
105	5	5th fin base temperature
106	6	5th fin tip temperature
107	7	6th fin base temperature
108	8	6th fin tip temperature
109	9	7th fin base temperature
110	10	7th fin tip temperature
111	11	8th fin base temperature
112	12	9th fin tip temperature
113	13	10th fin base temperature
114	14	A_1
115	15	A_2
116	16	A_3
117	17	B_1
118	21	B_2
119	22	B_3
120	20	C_1

Table 2.4c Data logger channel connections for the tube #4 (15 fins)

Channel No	**Thermocouple No**	**The point measured**
101	1	Heat transfer fluid inlet temperature
102	2	Heat transfer fluid outlet temperature
103	3	2nd fin tip temperature
104	4	3rd fin base temperature
105	5	7th fin base temperature
106	6	7th fin tip temperature
107	7	8th fin base temperature
108	8	8th fin tip temperature
109	9	9th fin base temperature
110	10	9th fin tip temperature
111	11	10th fin base temperature
112	12	14th fin base temperature
113	13	14th fin tip temperature
114	14	A_1
115	15	A_2
116	16	A_3
117	17	B_1
118	21	B_2
119	22	B_3
120	20	C_1

2.6 Computer System

During the experiments, the data scanned by the data logger were recorded on a personel computer. The values scanned every 30 seconds were be able to watched simultaneously on the computer screen by the help of HP Benchlink Data Logger software as shown in Figure 2.16. In addition, the inlet and the outlet temperatures of the heat transfer fluid were able to viewed graphically to ensure the inlet temperature to be constant.

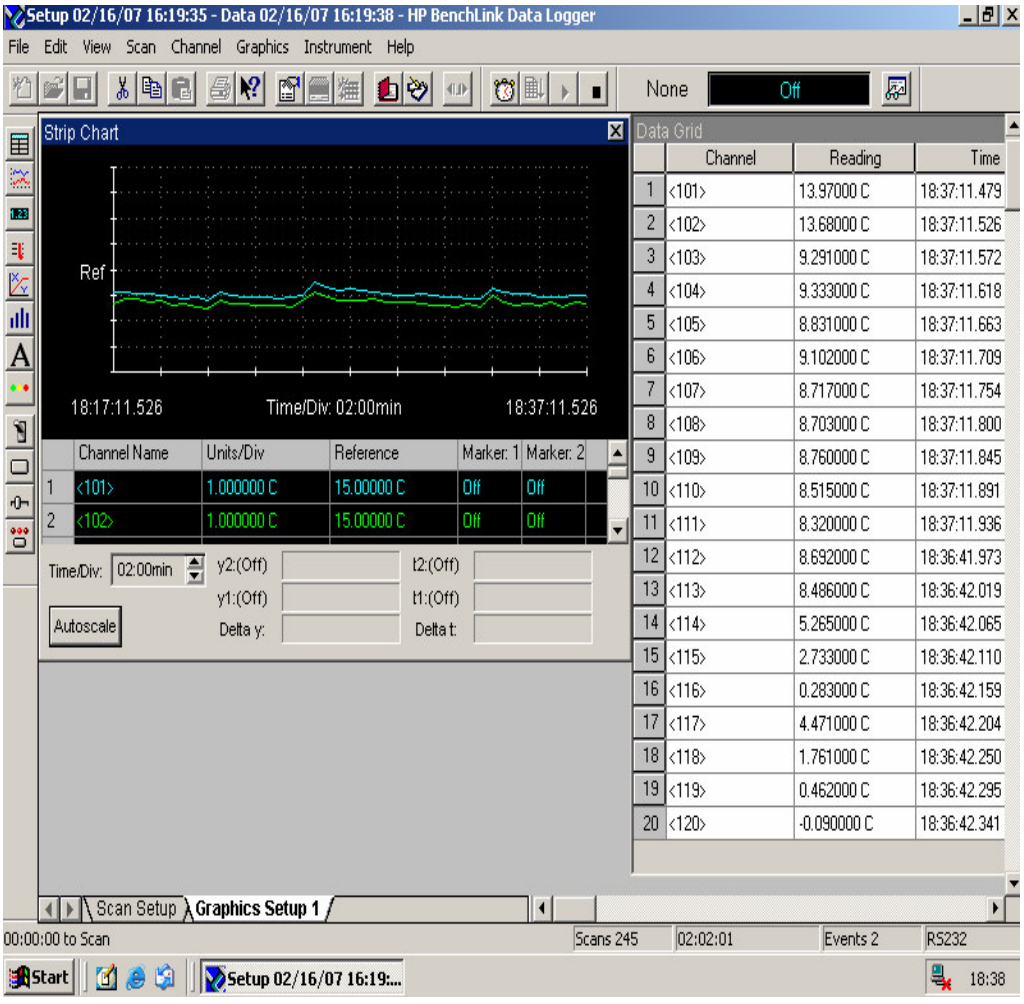

Figure 2.16 A view of HP Benchlink Data Logger software

CHAPTER THREE
EXPERIMENTAL PROCEDURE

3.1 Experimental Procedure

Firstly, the thermocouples were installed to one of the finned tubes to be tested for starting a particular set of experiments. Then the finned tube with the thermocouples on it was assembled to the storage tank The phase change material (water) was poured into the energy storage tank at a temperature of 0.3-0.8 °C. Then a precooling process was performed by pouring big ice pieces into the water. By applying this process, the temperature of the water was decreased more and became closer to 0°C. To make a more homogeneous temperature distribution in the water, the water with the ice pieces in it was stirred with a long stick. After this mixing process, all ice pieces were taken out carefully. The total amount of the water stored in the tank was at a level such that the test tube becomes oriented at the horizontal symmetry line of the tank. Ethyl alcohol at a predetermined flow rate was circulated through the system. After adjustment of the flow rate by the help of a beaker which is described in the previous chapter, the circulation of the alcohol was closed by the valves and the constant temperature bath was regulated for the desired inlet temperature which was -15°C. Then the ethyl alcohol at the specified inlet temperature was let abruptly into the test section by opening the outlet valve of the constant temperature bath. For each experiment, this procedure was repeated and a seven hours solidification process started. By the end of seven hours, the circulation of the alcohol was cut closing the outlet valve of the bath. For melting process, the inlet temperature of the ethyl alcohol was raised to 15°C. Then the circulation was started again. In a one day experimentation duration, all of these processes were performed for one different flow rate and different test tubes.

Inlet temperature of -15°C was studied for 5 different tubes: Two 7 finned (with different fin diameters - #1 and #2), one 11 finned (#3), one 15 finned (#4) and one finless tube (#5). In the previous chapter, all of these tubes were numbered for an easier expression. Three different values of Reynolds numbers were considered,

1000, 1500, 2000 of heat transfer fluid (ethyl alcohol) for each tube. The inlet and the outlet temperatures of the ethyl alcohol and the tested tube surface temperatures were measured and recorded at every thirty seconds by the data logger. As shown in Table 3.1, fifteen different experiments were carried out every single day. Each of these experiments consisted of solidification and melting parts.

Table 3.1 Experiments performed in this study

Test No	Tube No	Reynolds number	HTF inlet temperature (°C)	
			Solidification	Melting
1	#1	1000	-15	15
2	#1	1500	-15	15
3	#1	2000	-15	15
4	#2	1000	-15	15
5	#2	1500	-15	15
6	#2	2000	-15	15
7	#3	1000	-15	15
8	#3	1500	-15	15
9	#3	2000	-15	15
10	#4	1000	-15	15
11	#4	1500	-15	15
12	#4	2000	-15	15
13	#5	1000	-15	15
14	#5	1500	-15	15
15	#5	2000	-15	15

For solidification part of the experiments, experimental run lasted 7 hours. For all types of tubes this duration was the same. The images of solidification around the finned tube were taken at every 20 minutes periods. Some of these images for the tube #1 were shown in Figures 3.1a to 3.1c. For melting part, the experiment durations were different for all experiments. Since the finish of melting at any point around the ice was waited, the melting time was different for each experiment.

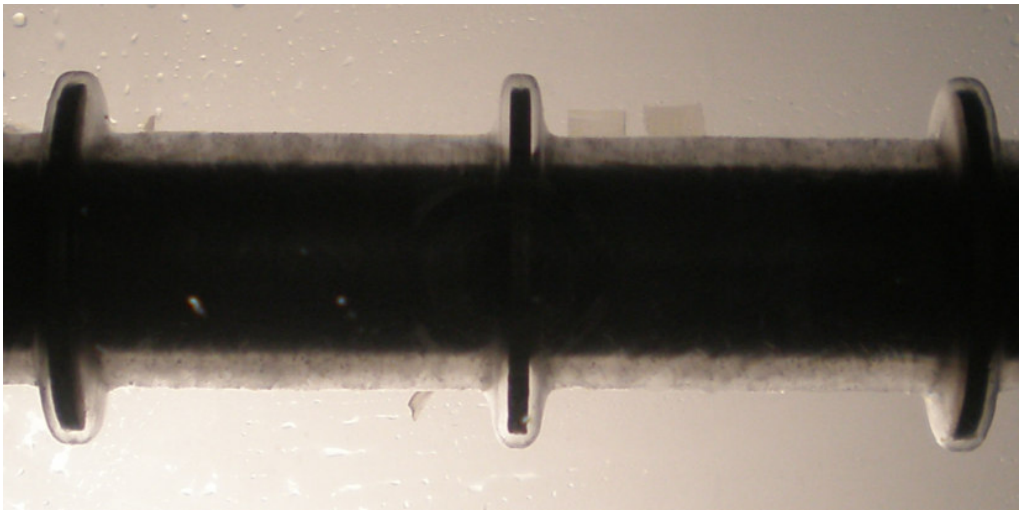

Figure 3.1a 20th minute of the solidification for the tube #1

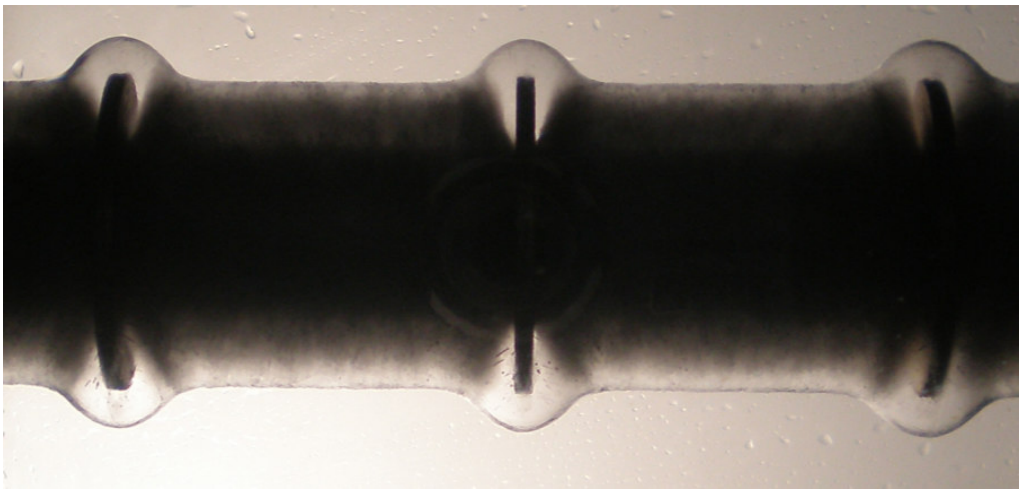

Figure 3.1b 60th minute of the solidification for the tube #1

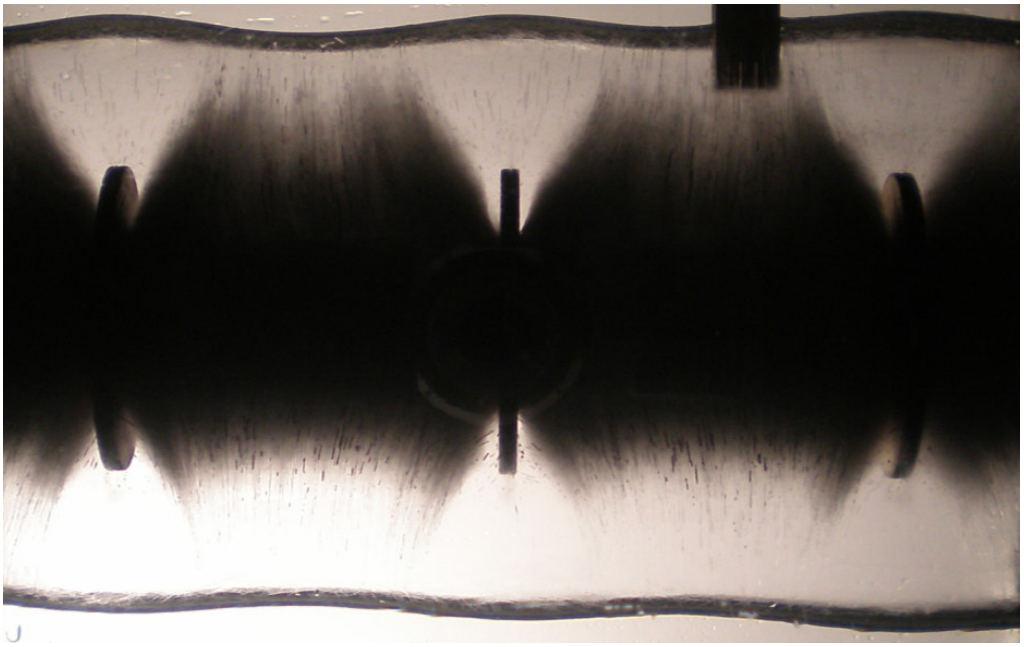

Figure 3.1c 7th hour of the solidification for the tube #1

After 7 hours of solidification, the temperature of the ethyl alcohol in the constant temperature bath was increased to 15°C for melting part of the experiments. The temperature of the thermocouples which were connected to the base of the middle fin (as shown in Figure 2.14 – A_1 and B_1 points) was waited to reach 0°C. Because those thermocoples were to measure the temperature of the tube surface. So the melting part of the experiment was started. Because of the convection factor, melting duration was shorter than the solidification process. So, to observe the changes of melting carefully, the photos were taken every 5 minutes for melting parts of the experiments. Some of these photos for the tube #1 were shown in Figure 3.2a and 3.2b.

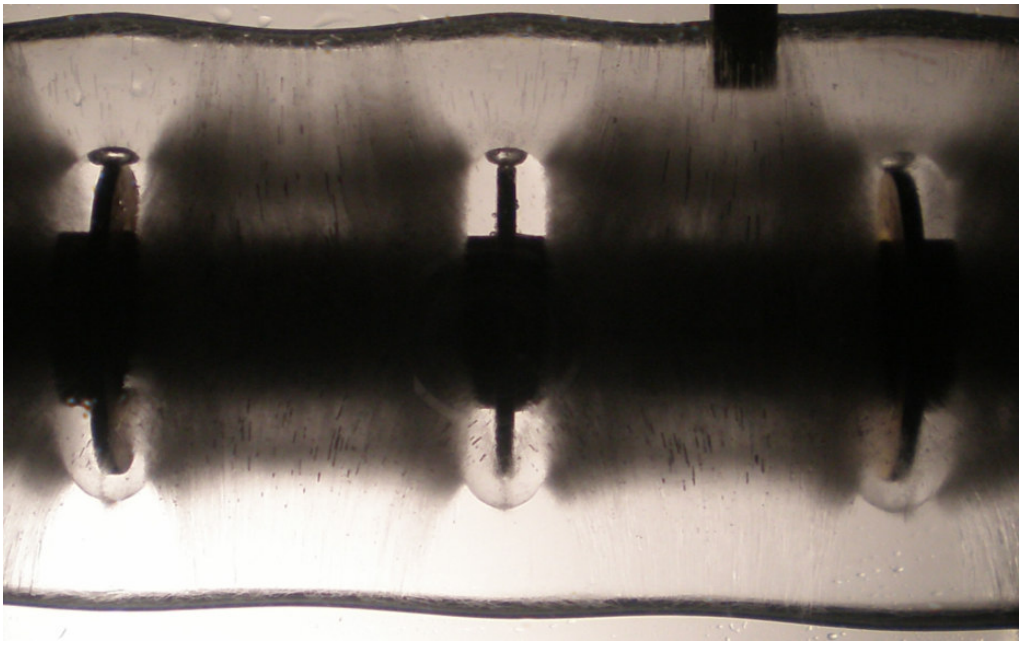

Figure 3.2a 60th minute of the melting for the tube #1

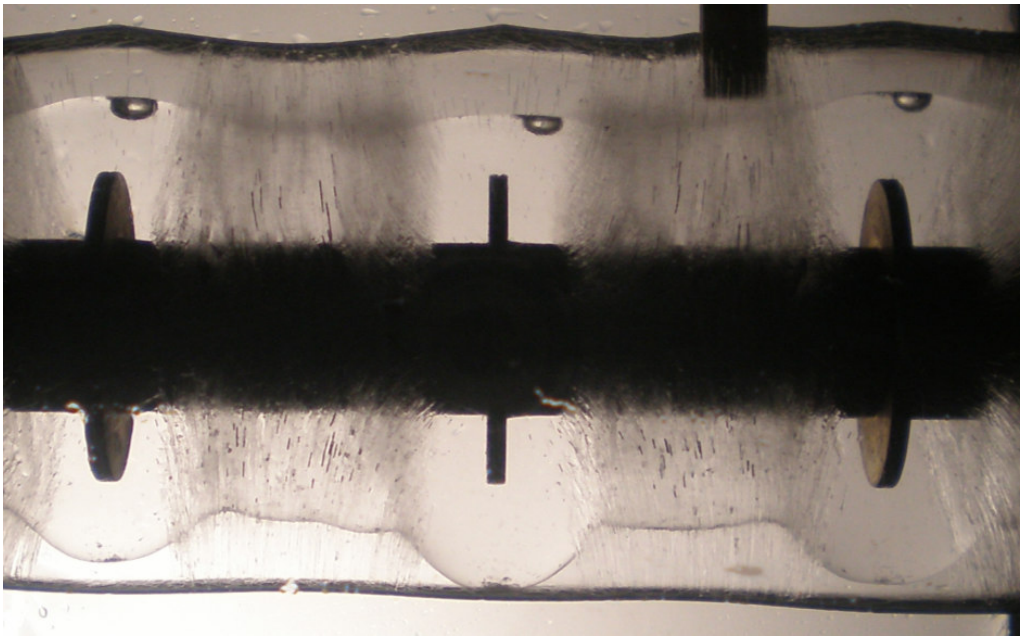

Figure 3.2b 3rd hour of the melting for the tube #1

To take the photos, the covers at the front and the back openings of the plexiglass surfaces were taken out. The white light rays from a lamp were reflected into the test section by the help of a white screen. Thus the essential enlightment for taking clear pictures of the solidification and melting fields around the tube was provided. As

shown in Figure 3.3, the digital camera was mounted at the center of the front window of the test section, and was directed perpendicular to the approaching light rays. Every 20 minutes for the solidification process and every 5 minutes for the melting process, the camera took the images of ice around the tube at the size of 2816x2112 pixels. Then these images were transmitted to a personal computer.

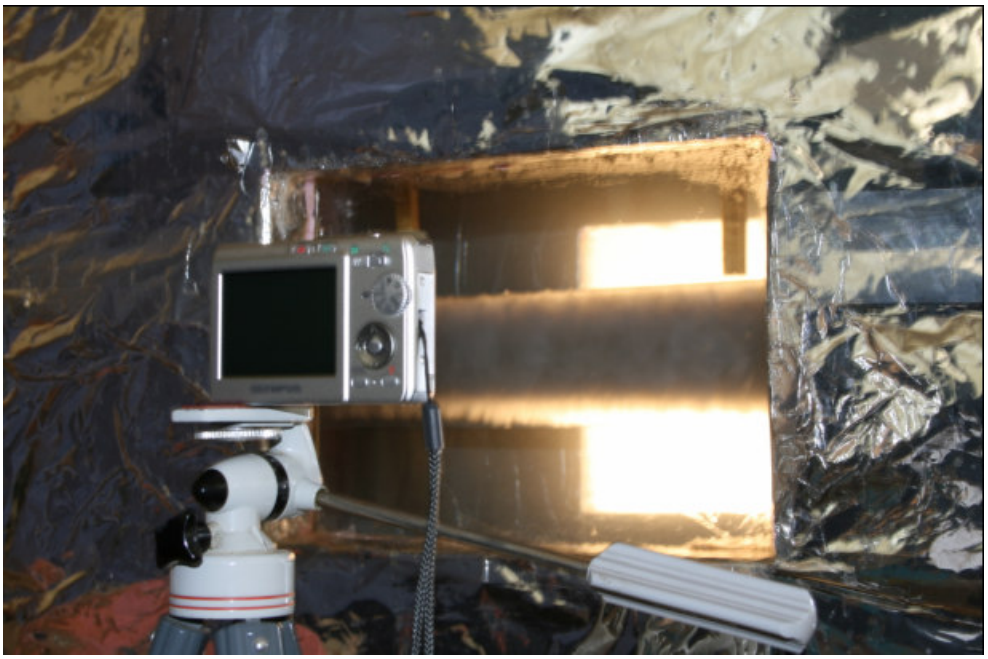

Figure 3.3 The camera position at the front of the view window of the energy storage unit

3.2 Determination of Charged and Discharged Cold Thermal Energy

For the solidification part of the experimental run, the amount of negative energy stored comprises latent heat of ice and sensible heat of both ice and water. So, the total energy stored is,

$$E_{total} = E_{sensible,water} + E_{sensible,ice} + E_{latent,ice} \tag{3.1}$$

where,

$$E_{sensible,water} = m_{water} c_{p,water} \left(T_i - T_{water} \right) \tag{3.2}$$

$$E_{sensible,ice} = m_{ice} c_{p,ice} \left(T_{ice} - T_{fr} \right) \tag{3.3}$$

$$E_{latent,ice} = m_{ice} L \tag{3.4}$$

During the experiment, solidified and melted diameters of the phase change material and temperatures were collected periodically for computation of the latent heat of ice and sensible heat of water and ice. In the process of solidification, equations (3.3) and (3.4) were used in order to determine the stored energy. Since the initial temperature of the water, T_i, was almost equal to zero, equation (3.2) was not used for computing the stored cold energy. Nevertheless, for sensible heat of ice, the equation (3.3) could not be used directly. Because, a new equation was to be derived as a function of the finned tube wall temperature, T_w, and solidified phase change material radius, r_{ice}, at a certain instant of time. The derivation of this kind of equation is as follows (Acar, 2003):

Logarithmic temperature distribution in a cylindrical system is described as,

$$\frac{q}{l} = \frac{2\pi k \left(T_1 - T_2 \right)}{\ln \frac{r_2}{r_1}} \tag{3.5}$$

Conduction in the solid phase change material is written as,

$$q = -k \left(2\pi r l \right) \frac{dT}{dr}$$

$$\frac{q}{2\pi k l} \frac{dr}{r} = -dT \qquad \frac{q}{2\pi k l} \int_{r_{po}}^{r} \frac{dr}{r} = -\int_{T_w}^{T} dT \qquad \frac{q}{2\pi k l} \ln \frac{r}{r_{po}} = T_w - T$$

Because the temperature at solid-liquid interface of the phase change material is equal to zero,

$$\frac{q}{2\pi k l} \ln \frac{r_{ice}}{r_{po}} = T_w \tag{3.6}$$

After combining the equations (3.5) and (3.6),

$$\frac{T}{T_w} = 1 - \frac{\left(\ln r / r_{po}\right)}{\left(\ln r_{ice} / r_{po}\right)}$$

Sensible heat of ice may be written as,

$$E_s = \int_{r_{po}}^{r_{ice}} \rho c \left(2\pi r dr dx\right)\left(T - T_{fr}\right) = 2\pi\rho c \left(\int_{r_{po}}^{r_{ice}} rTdr \right) dx = 2\pi\rho c T_w dx \int_{r_{po}}^{r_{ice}} r \left(1 - \frac{\left(\ln r_{po} / r\right)}{\left(\ln r_{ice} / r_{po}\right)} \right) dr$$

Integration of the above equation yields the sensible heat stored in unit length of the phase change material (Acar, 2003).

$$\frac{E_s}{\Delta x} = \sum_{i=1}^{n} \rho\pi c T_w \left[\left(r^2_{ice,i} - r^2_{po,i} \right) + \frac{r^2_{ice,i}}{2\ln\left(r_{ice,i} / r_{po}\right)} \left(1 - 2\ln\frac{r_{ice,i}}{r_{po}} - \left(\frac{r_{po}}{r_{ice,i}} \right)^2 \right) \right] \qquad (3.7)$$

During the melting process, the discharged cold thermal energy was computed using the equations (3.2) and (3.4). As in the solidification process, the equation of the sensible heat of water could not be used directly. So equation (3.7) was again used for computing the sensible heat. Melting area radii were applied in that equation instead of the ice radii.

Taking into consideration the equations (3.1) to (3.7), an exact computation of the mass of ice which was took shape during the solidification process of the experimental run was an extremely important problem and must be done precisely. Luminous images which clearly showed the boundaries of the ice formed around the finned tube were obtained. By the help of a software (AutoCad 2007), vertical grid lines oriented with a horizontal distance of δx=1 mm were generated on the pictures

as shown in Figure 3.4a and 3.4b for the solidification and melting processes respectively.

The diameters of the solidified or melted phase change material were measured at every 1 mm of the module by measuring vertical distances between the ice-boundary grid-line intersections. Then these measured diameter values were converted to the actual diameters by proportioning with the fin diameter of that image.

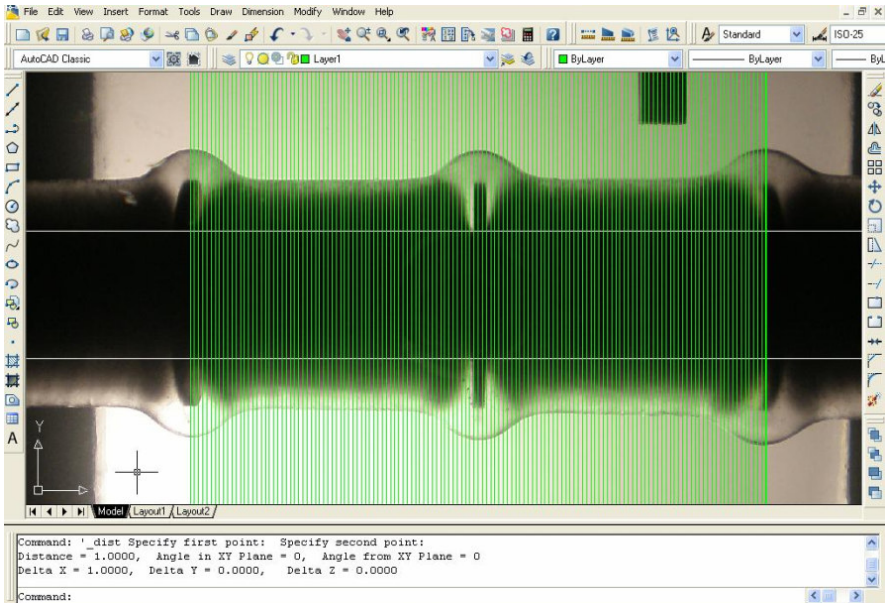

Figure 3.4a Vertical grid lines formed in the software Autocad 2007 for computing solidified ice diameters

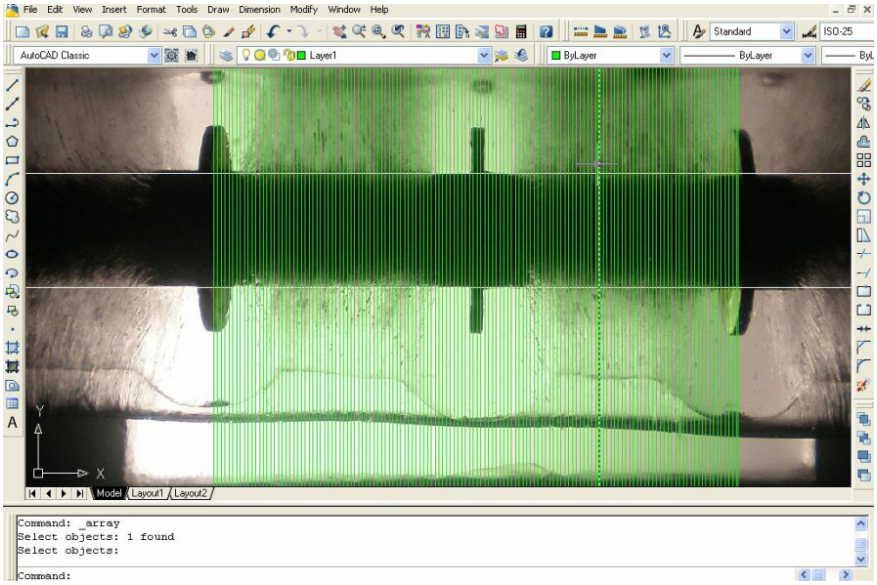

Figure 3.4b Vertical grid lines formed in the software Autocad 2007 for computing melted ice diameters

Considering diameter at a certain location i, the volume of ice formed at the module of the tested tube becomes,

$$V_{ice,cell} = \frac{\pi}{4}\sum_{i_1}^{i_2} d_i^2 \delta x - V_{tube,cell} \tag{3.8}$$

where i_1 and i_2 are the vertical grid lines on the left and right side of the module as shown in Figures 3.4a and 3.4b.

For the experiments, it was assumed that the amount of ice formed or melted at each module is at the same amount as the middle module of the tubes which was computed during the study. So, the volume of ice formed around the whole finned tube surface up to that instant time was,

$$V_{ice} = V_{ice,cell}\frac{l}{2(w+t)} \tag{3.9}$$

where l is the length of the tested tube, w is the space between the fins and t is the thickness of the fins (Acar, 2003). For the finless tube, the middle module was selected between the same points where the fins were existed for the finned tubes #1 or #2.

After determining the solidified and melted volumes of the water, the masses of these volumes were computed. Eventually the latent energies could be computed.

CHAPTER FOUR
EXPERIMENTAL RESULTS

The stored energy values were calculated for each experiment as described in the previous chapter. The stored energy values were displayed as a function of time under the effects of some parameters which are the fin density, the fin diameter and Reynolds numbers of the heat transfer fluid. Because of the breakdown of the constant temperature bath, experiments could not be completed for the tube #4. For this tube, only Re=1000 solidification-melting parts and Re=1500 solidification part were able to be experimented.

In Figures 4.1a to 4.1e, the effects of Reynolds numbers of the heat transfer fluid on the total stored energy were shown. Those figures were for solidification parts of the experiments. For the most of the experiments, it can be seen from the figures that increase of Reynolds number means increase of the solidification and stored cold energy. Since the breakdown occured in the constant temperature bath during the experiment on the tube #4, the values for Re=2000 could not be get for that experiment. Because of that, as shown in Figure 4.1d, stored energy change with time is seen only for Re=1000 and Re=1500. For both Reynolds numbers, it is seen that the values of the stored energy is almost identical. Another unexpected result happened for the tube #2 which is seen at Figure 4.1b. The stored energy is nearly more for Re=1500 compared to Re=2000.

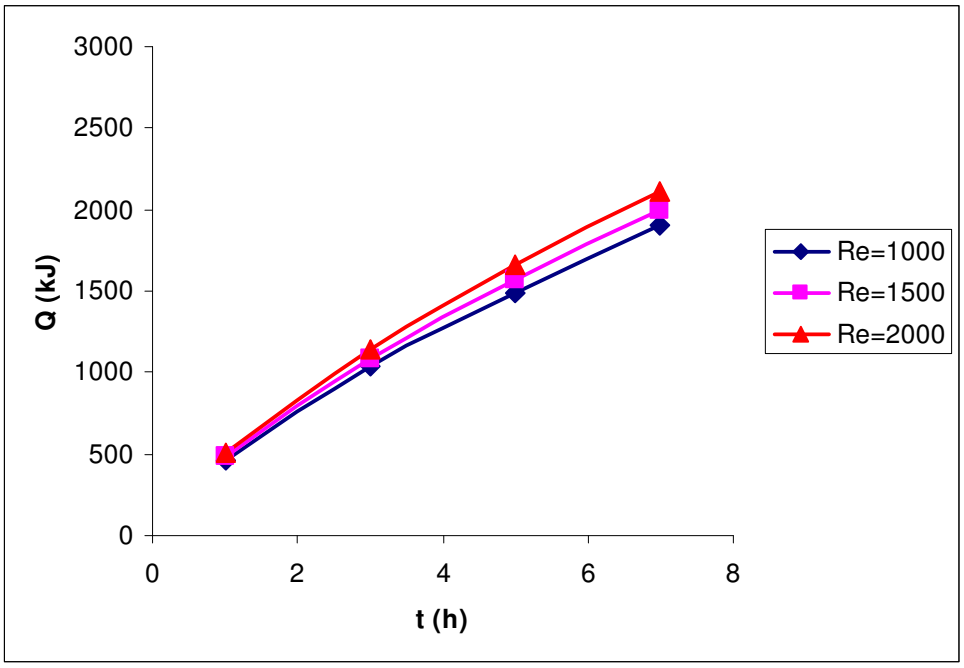

Figure 4.1a The effect of Reynolds number on total stored energy for the tube #1 during solidification

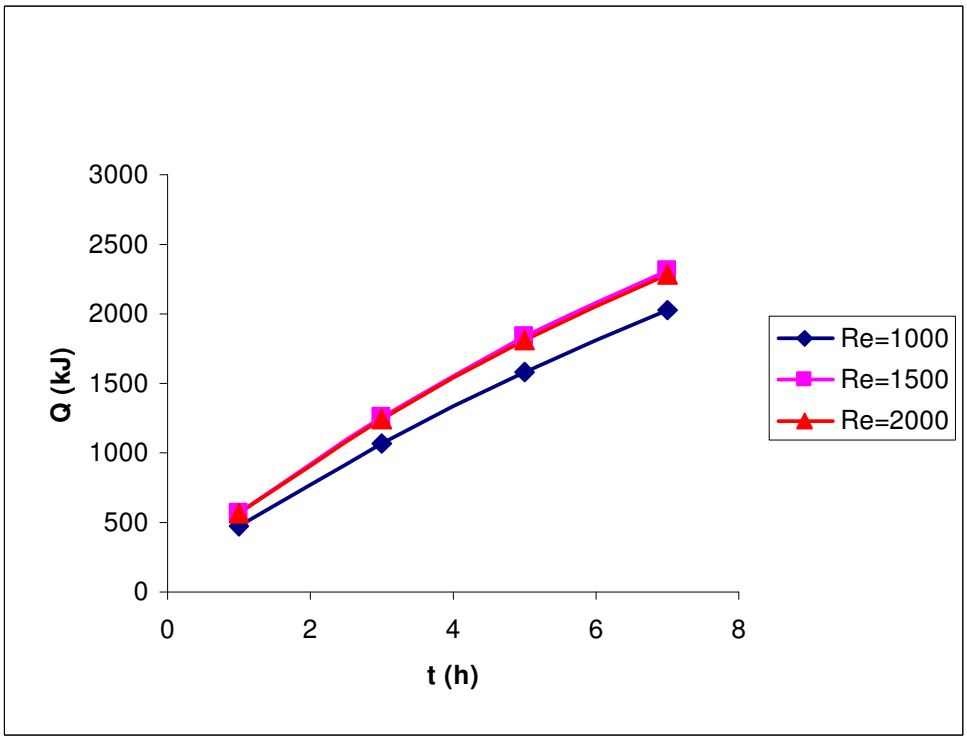

Figure 4.1b The effect of Reynolds number on total stored energy for the tube #2 during solidification

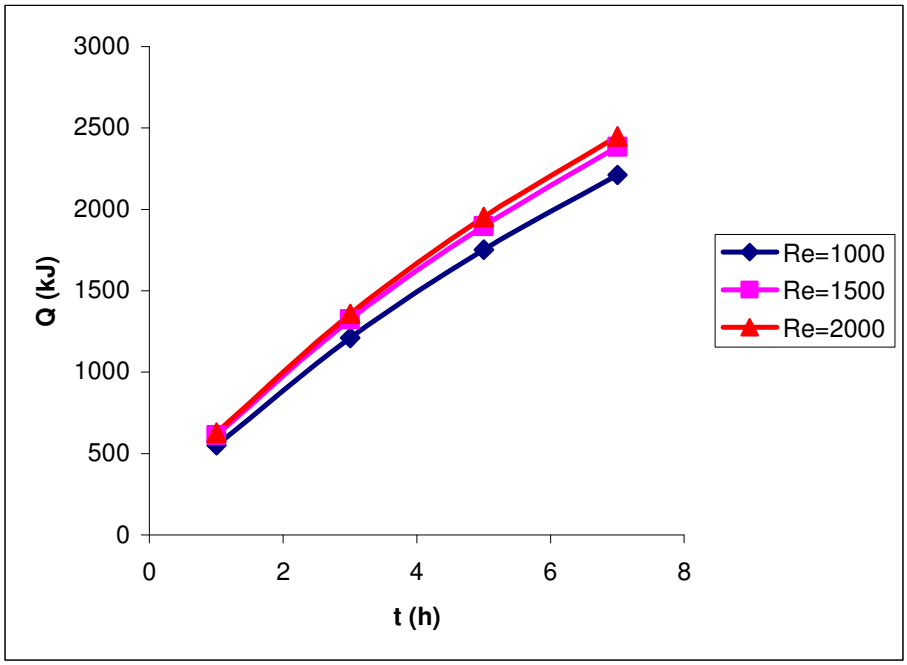

Figure 4.1c The effect of Reynolds number on total stored energy for the tube #3 during solidification

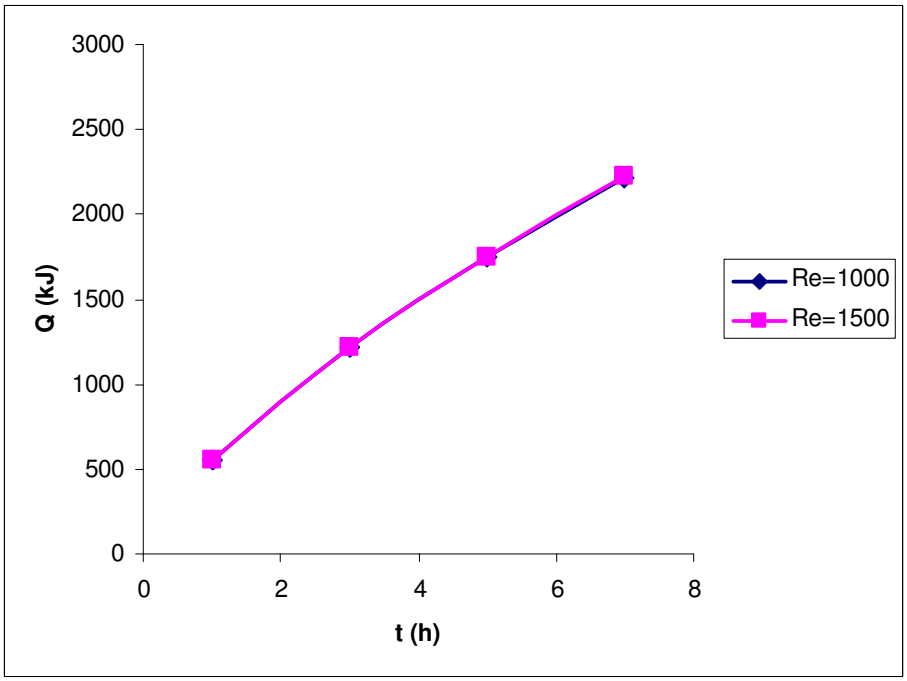

Figure 4.1d The effect of Reynolds number on total stored energy for the tube #4 during solidification

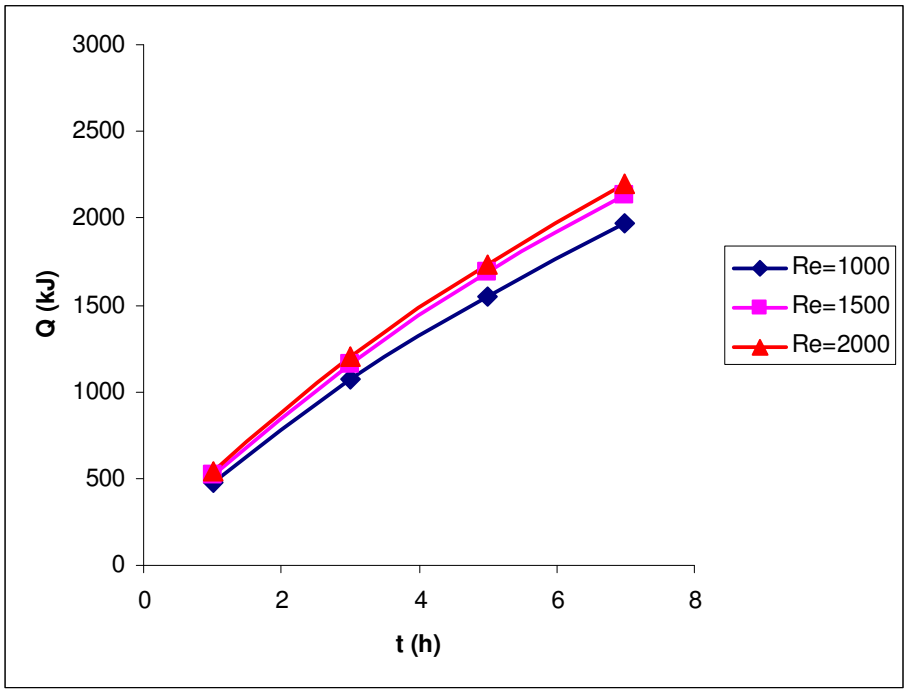

Figure 4.1e The effect of Reynolds number on total stored energy for the tube #5 during solidification

In Figures 4.2a to 4.2d those effects were shown for melting section. Because of the breakdown of the constant temperature bath during experiments cited before, the comparison could not be made for the tube #4 for which only values for Re=1000 were obtained. The complex nature of the melting can be clearly seen from these figures. While the duration of all solidification sections was kept constant as 7 hours, the melting duration was different for all experiments. Because, at the beginning of the melting section of the experiments which followed the solidification section, the ice volume was also different for each experiment. Eventually each melting experiment lasted for dissimilar duration. Figures show that Reynolds number also effects the melting period. The effect is in the same direction as is in solidification. As we increase the Reynolds number, the result will be an increase in the melted volume and the discharged cold energy. For those series of experiments, the unexpected result was for the tube #1 which is shown in Figure 4.2a. It can be seen that the least discharged cold energy happened for Re=2000.

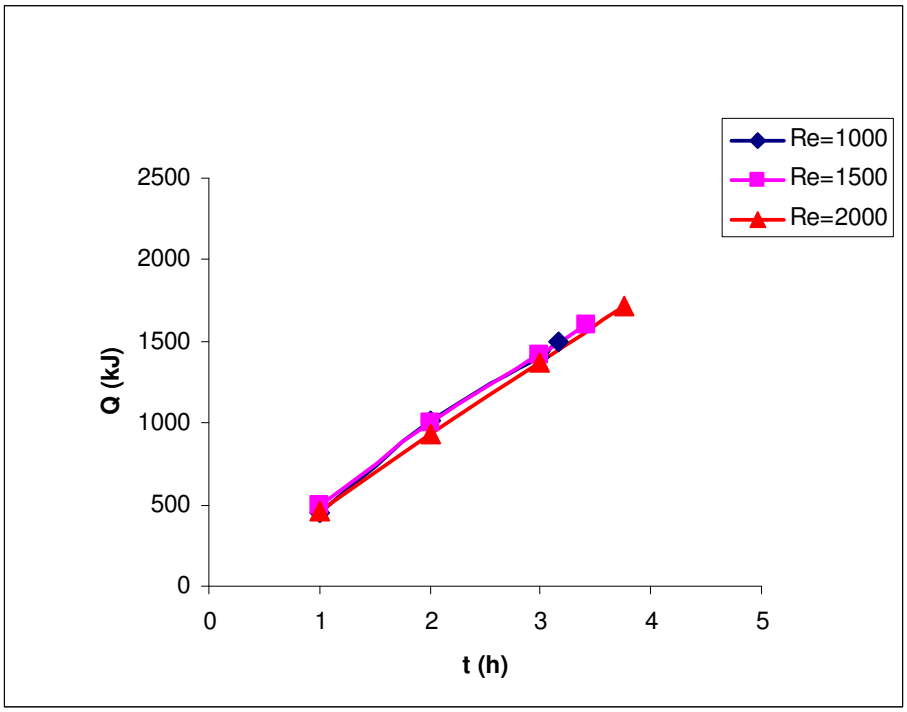

Figure 4.2a The effect of Reynolds number on discharging of total stored energy for the tube #1 during melting

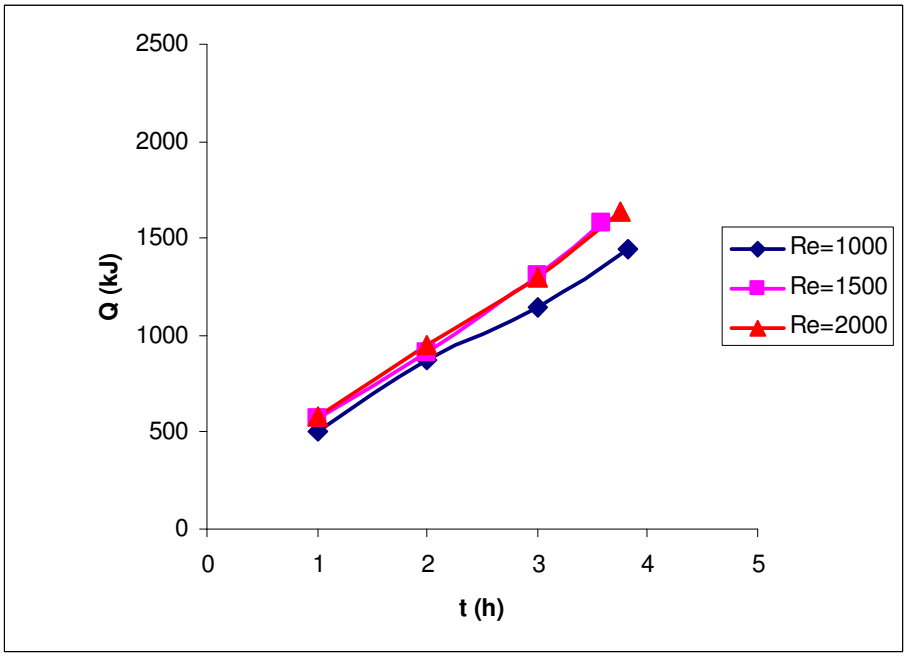

Figure 4.2b The effect of Reynolds number on discharging of total stored energy for the tube #2 during melting

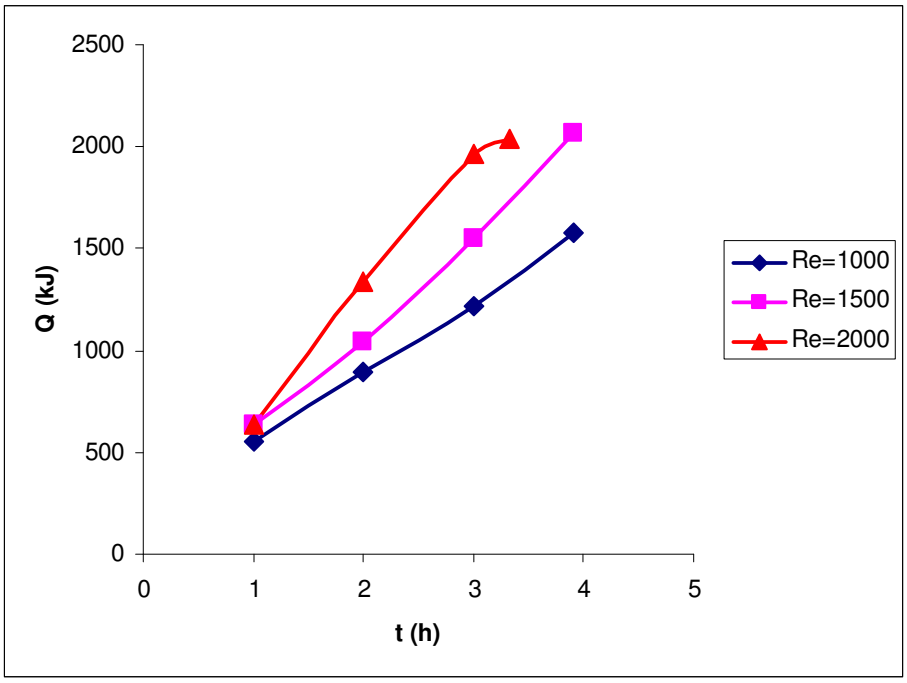

Figure 4.2c The effect of Reynolds number on discharging of total stored energy for the tube #3 during melting

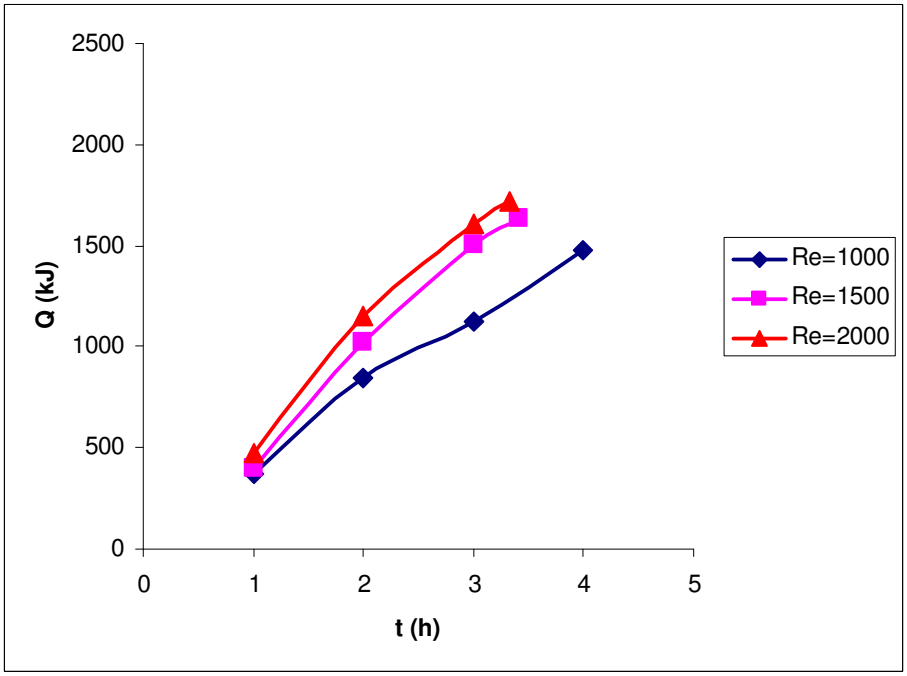

Figure 4.2d The effect of Reynolds number on discharging of total stored energy for the tube #5 during melting

For a specific value of the fin density and Reynolds number of the heat transfer fluid (Re=1000 and Re=2000), the effect of the fin diameter on the stored and discharged cold energy is indicated in Figures 4.3a and 4.3b for solidification and melting sections respectively. The tubes #1 and #2 which have same fin density is used for this process. In Figure 4.3a, for solidification, it is clearly seen that the increase of the fin diameter increases the stored cold energy. Especially for higher Reynolds numbers, this increase becomes higher. For example, when Re=2000, the difference of the stored energy between D_f=54 mm and D_f=64 mm is more apparent. The results of the experiments show that it is more complex for melting. As shown in Figure 4.3b, for Re=1000 the situation is just the opposite in melting part of the experiments. The increase in the fin diameter does not increase the discharged cold energy. But for Re=2000, the values are more closer for both fin diameters.

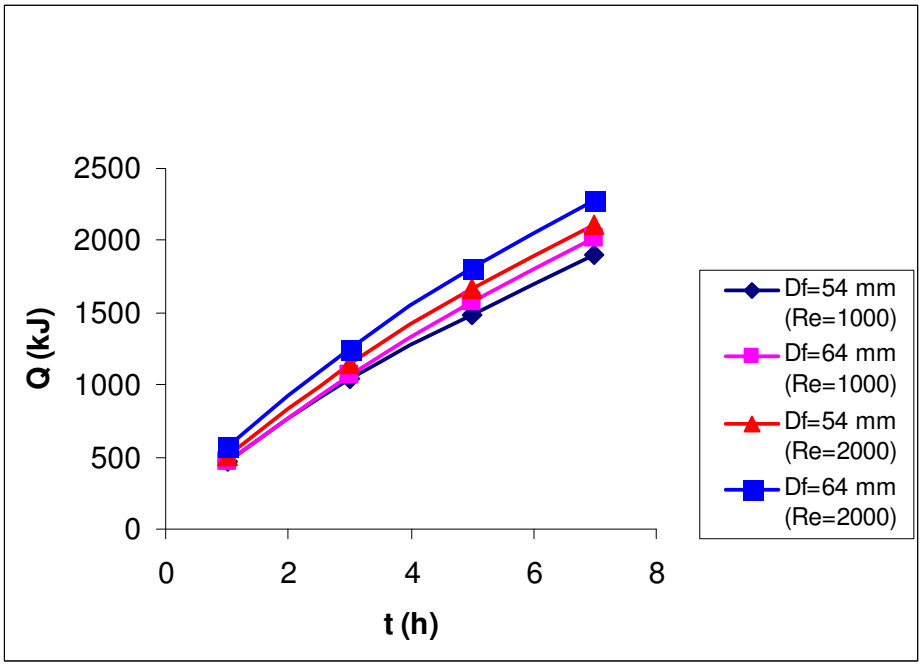

Figure 4.3a The effect of the fin diameter on total stored energy for the tubes #1 and #2 during solidification

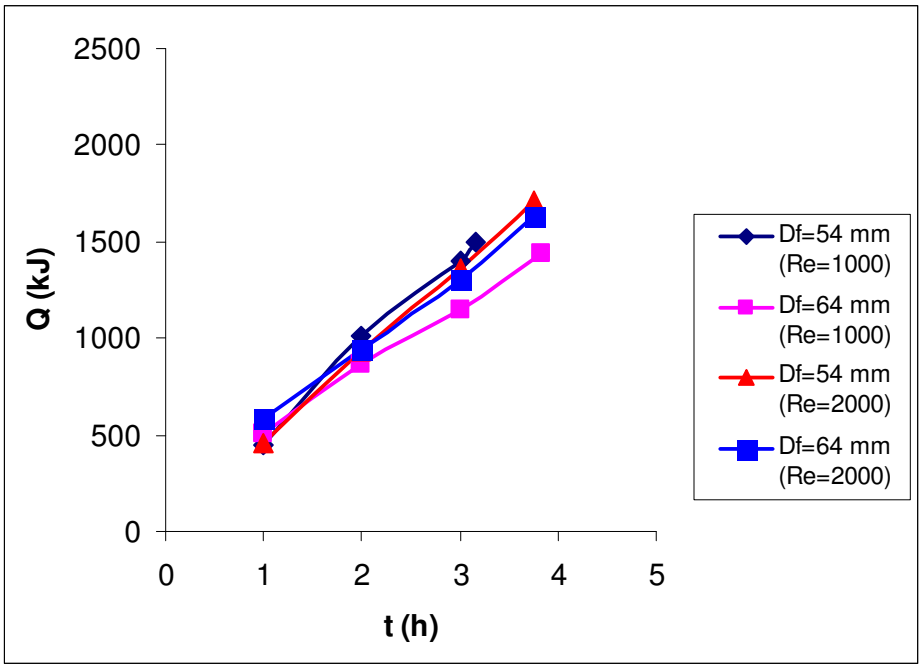

Figure 4.3b The effect of the fin diameter on discharging of total stored energy for the tubes #1 and #2 during melting

In Figures 4.4a to 4.4c, effect of the fin densitiy on the stored cold energy is displayed for different Reynolds numbers of the heat transfer fluid and constant fin diamater. The results show that the stored energy generally increases with the increase of the fin density. For all Reynolds numbers, the least energy was stored for the tube #1 which has 7 fins. It is expected that would be the finless tube but all experiments show the same result. Although the tube #4 has the biggest fin density which is 15 fins, as can be seen in Figure 4.4b, for Re=1500, the most energy storage occured for the tube #3 which has 11 fins. This is an exception for the general nature of the fin density-stored energy relation.

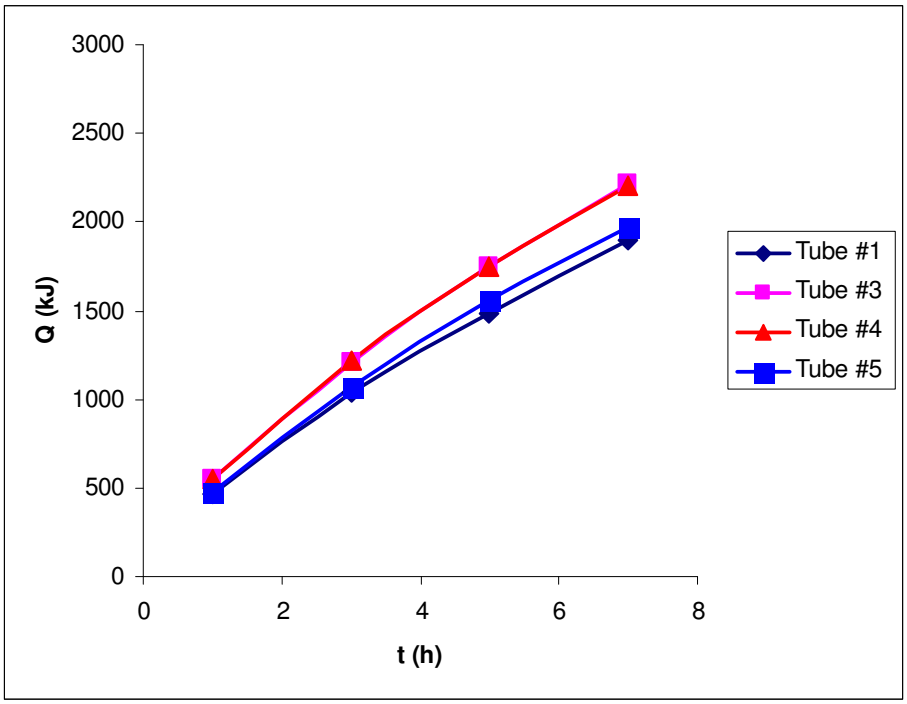

Figure 4.4a The effect of the fin density on total stored energy for Re=1000 during solidification

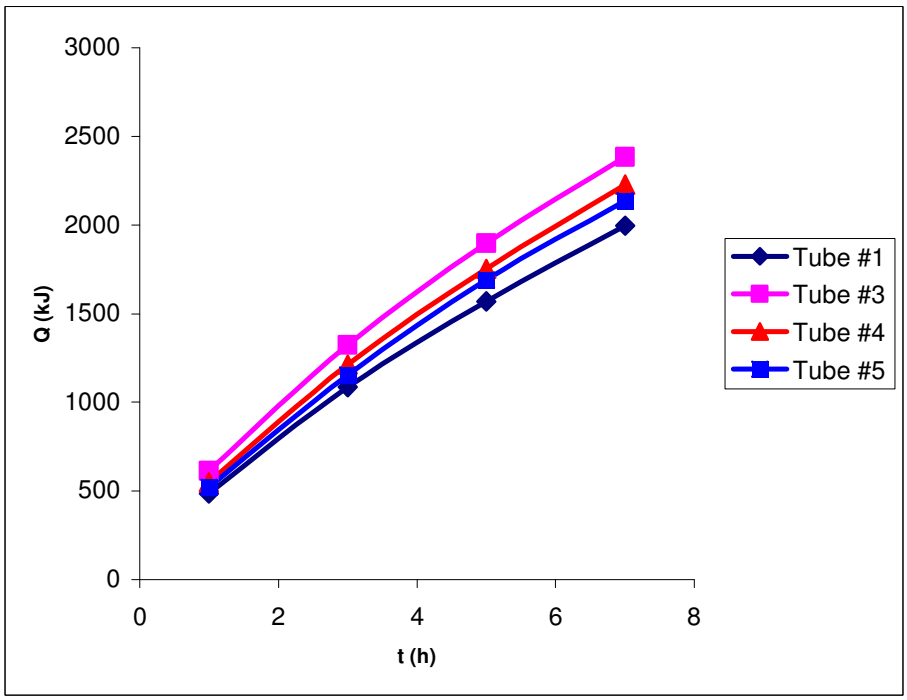

Figure 4.4b The effect of the fin density on total stored energy for Re=1500 during solidification

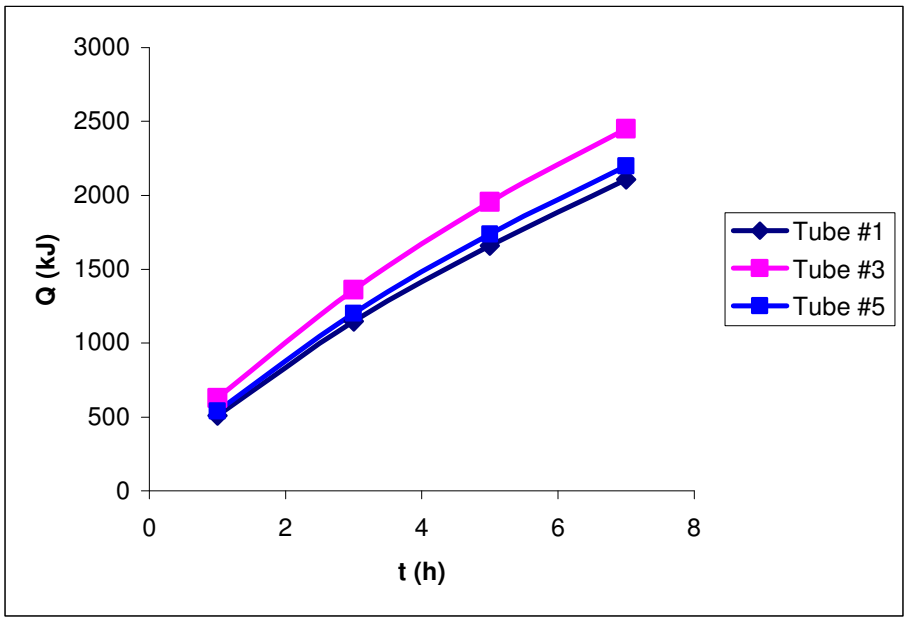

Figure 4.4c The effect of the fin density on total stored energy for Re=2000 during solidification

Effect of the fin density on discharge of the stored cold energy is indicated for different Reynolds numbers of the heat transfer fluid and constant fin diamater in Figures 4.5a to 4.5c. It can be seen that the relation between the fin density and the energy resembles the solidification results. But it must be noted that, at the first hours of the melting, the fin densitiy-discharged cold energy relationship is more stable. More energy discharges as the fin density increases for the first parts of the melting.

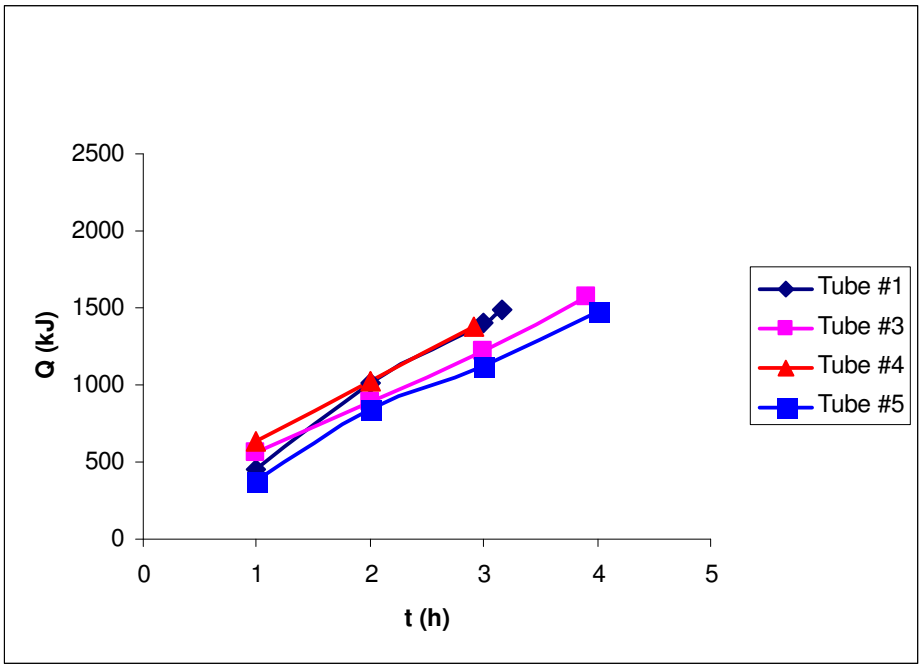

Figure 4.5a The effect of the fin density on discharging of total stored energy for Re=1000 during melting

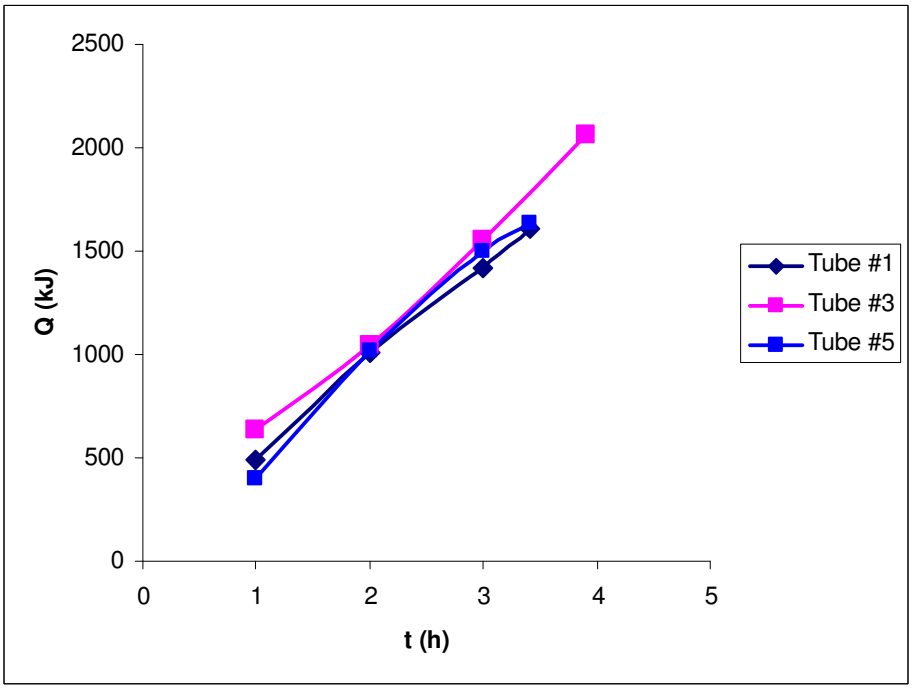

Figure 4.5b The effect of the fin density on discharging of total stored energy for Re=1500 during melting

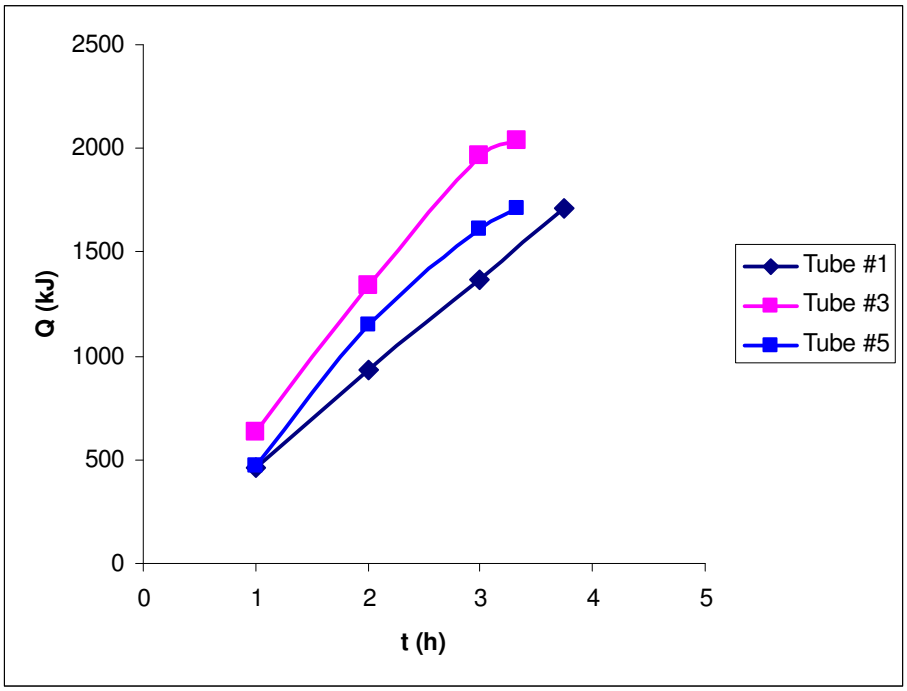

Figure 4.5c The effect of the fin density on discharging of total stored energy for Re=2000 during melting

The values of stored and discharged energy were listed in the Appendices section which is at the end of the thesis.

CHAPTER FIVE
CONCLUSIONS

In this study, the effects of the fin density, the fin diameter and Reynolds numbers of the heat transfer fluid on storing latent cold energy were investigated experimentally. These effects were observed for both charging and discharging of the cold energy. For this purpose, a series of experiments were performed and the results were recorded. The parameters that were changed during the experiments were as follows:

- Reynolds number of the heat transfer fluid,
- the fin diameter,
- the fin spacing.

It was known that the parameters like time and the inlet temperature of the heat transfer fluid were another effective factors on the thermal storage in the experiments. No doubt as the time elapsed, the amount of energy charging or discharging was increased. The effect of the inlet temperature of the heat transfer fluid was not investigated in this study. For each experiment -15°C was the inlet temperature during the charging of the cold energy. This value was increased to 15°C for melting process in each of the experiments. The inlet temperature would effect the energy storage primarily, especially on the speed of solidification and melting.

As described in the previous chapters, five different shaped tubes were used in the tests in order to figure out the effects of the fin diameter and spacing on the energy storage. The Reynolds number of the heat transfer fluid was altered by the valves in the experimental setup to be Re=1000, Re=1500 and Re=2000.

It was clearly seen that the increase of the flow Reynolds number of the heat transfer fluid increased the stored energy during solidification of the phase change material. Same result was occured for the melting process. But for the tube #1 the results were unexpected and contrary.

The effect of the fin diameter was investigated on the tubes #1 and #2 which have same fin density that was seven tubes for whole tube. For the same Reynolds numbers, increase of the fin diameter increased the stored energy during solidification. Especially at higher Reynolds numbers, that effect was more apparent. Those results were also valid for the first hours of the melting processes. But in the following hours of the experiments, these tendencies shifted completely for each of the flow rates.

The experiments brought out some interesing results about the effect of the fin density on the energy storage. As expected, increasing of the fin density resulted in more energy storage during solidification process. But, especially at high Reynolds numbers, the amount of the stored energy for the tube #5 which was finless was higher than for the tube #1 which had 7 fins for the same length. After this point, increasing the fin density more caused more energy storage. This result may show that increasing the heat transfer area by the use of the fins effects the amount of the stored energy only using more than a specific number of fins. For the melting processes, the results were more complicated than the ones of the solidification again. This result was seen for all of the experiments. The effect of the natural convection on this results certainly can not be forgotten at this point. At the first hours of the melting, it was seen that the amount of the discharged cold energy were increased by the increase of the fin density. But as the time passed, some small changes happened again.

By looking the general results of the experiments, it was seen that some unexpected conclusions compared to the general tendencies of the results existed. There are many factors such as instrumental manufacturing errors, human nature reading errrors, environmental condition effects or calibration errors that may cause some diversions in the experiments. At some moments of the tests, these diversions can happen because of the factors such as thermocouples, data logger system, inlet temperature measurement, surface temperature measurement, flow rate reading, system leakages and so on.

As a conclusion, in this study the effects of the fin diameter, fin density and the flow Reynolds number of the heat transfer fluid on charging and discharging of the cold thermal energy using a phase change material around a finned tube were investigated experimentally and the results were compared. The results generally showed that the increase of the fin diameter, fin density and Reynolds number increased the amount of charging and discharging cold thermal energy during solidification and melting processes respectively.

NOMENCLATURE

c_p	specific heat (J kg^{-1} K^{-1})
D	diameter (m)
E	energy charged or discharged
k	thermal conductivity (W m^{-1} K^{-1})
l	length of tube (m)
L	specific latent heat (J kg^{-1})
m	mass (kg)
t	fin thickness (m)
T	temperature (K)
w	fin spacing (m)
Q	total charged or discharged energy (J)

Greek Symbols

α	thermal diffusivity (m^2 s^{-1})
μ	dynamic viscosity (kg m^{-1} s^{-1})
ρ	density (kg m^{-3})

Subscripts

f	fin
i	initial condition or inner surface of tube
o	outer surface of tube
p	pipe
s	sensible
w	wall
fr	freeze point

REFERENCES

Acar, M. A. (2003). Study of finned tube thermal energy storage systems. M. Sc thesis. İzmir: Graduate School of Natural and Applied Sciences of Dokuz Eylül University.

Akgün, M., Aydın, O., & Kaygusuz, K. (2006). Experimental study on melting/solidification characteristics of a paraffin as PCM. *Energy Conversion & Management, 48*, 669-678

ASHRAE, (1987). *Thermal Storage*, HVAC Handbook. Chapter 46.

Bathelt, A. G., & Viskanta, R. (1981). Heat transfer and interface motion during melting and solidification around a finned horizontal sink/source. *Journal of Heat Transfer, 103,* 720-726.

Bellecci, C., & Conti, M. (1993). Phase change thermal storage: Transient behaviour analysis of a solar receiver/storage module using the enthalpy method. *International Journal of Heat Mass Transfer, 36,* 2157-2163.

Cao, Y., & Faghri, A. (1991a). A PCM/forced convection transient analysis of energy storage systems with annular and countercurrent flows. *Journal of Heat Transfer ASME, 113,* 37-42

Cao, Y., & Faghri, A. (1991b). Performance characteristics of a thermal energy storage module: A transient PCM/forced convection conjugate analysis. *International Journal of Heat Mass Transfer, 34,* 93-101.

Cao, Y., & Faghri, A. (1992). A study of thermal energy storage system with conjugate turbulent forced convection. *Journal of Heat Transfer ASME, 114,* 1019-1027.

Chemical Engineering Research Information Center. Retrieved May 12, 2007, from http://www.cheric.org/research/kdb/hcprop/cmpsrch.php

Erek, A. (1999). Phase change around finned horizontal cylinder: A conjugate problem. Ph. D. Thesis, Graduate School of Natural and Applied Sciences of Dokuz Eylül University, İzmir.

Erek, A., İlken, Z., & Acar, M. A. (2005). Experimental and numerical investigation of thermal energy storage with a finned tube. *International Journal of Energy Research, 29,* 283-301.

Ermiş, K., Erek, A., & Dinçer, İ. (2007). Heat transfer analysis of phase change process in a finned-tube thermal energy storage system using artificial neural network. *International Journal of Heat and Mass Transfer, 50,* 3163-3175.

Ismail, K. A. R., & Alves, C. L. F. (1986). Analysis of the shell-and-tube PCM storage system. *Proceedings of the 8th International Heat Transfer Conference,* 1781-1786.

Ismail, K. A. R., Henriquuez, J. R., Moura, L. F. M., & Ganzarolli, M. M. (2000). Ice formation around isothermal radial finned tubes. *Energy Conversion & Management, 41,* 585-605.

Kays, W. M. (1966). *Convective heat and mass transfer*. USA: McGraw-Hill, Inc.

Lacroix, M. (1993). Study of the heat transfer behaviour of a latent heat thermal energy storage unit with a finned tube. *International Journal of Heat Mass Transfer, 36,* 2083-2092.

Padmanabhan, P. V., & Khrishna, M. V. (1989). Outward phase change in a cylindirical annulus with axial fins on the inner tube. *International Journal of Heat Mass Transfer, 29,* 1855-1868.

Sasaguchi, K., Sakamoto, Y. (1989). Effects of natural convection on melting of a phase change material around a finned tube. *Transactions JSME, 55* (513), 1418-1425.

Sparrow, E. M., Larson, E. D., & Ramsey, J. M. (1981). Freezing on a finned tube for either conduction-controlled or natural convection-controlled heat transfer. *International Journal of Heat Mass Transfer, 24,* 273-284.

Zhang, Y., & Faghri, A. (1996a). Analytical solution of thermal energy storage system with conjugate laminar forced convection. *International Journal of Heat Mass Transfer, 39,* 717-724.

Zhang, Y., & Faghri, A. (1996b). Heat transfer enhancement in latent heat thermal energy storage system by using the internally finned tube. *International Journal of Heat Mass Transfer, 39,* 3165-3173.

APPENDICES

The amount of stored or discharged energy values which were computed for various moments of the experiments were shown in the tables below:

Table A.1 Stored cold energy values during solidification for different types of tubes

STORED COLD ENERGY DURING SOLIDIFICATION (kJ)			
Time	**The Tube with 7 fins (small diameter)**		
	Re=1000	**Re=1500**	**Re=2000**
1 h	465.1233	487.7256	507.7508
3 h	1042.0899	1085.5919	1147.7507
5 h	1489.2954	1569.2243	1660.6869
7 h	1899.6531	1997.3825	2107.6186
Time	**The Tube with 7 fins (big diameter)**		
	Re=1000	**Re=1500**	**Re=2000**
1 h	473.7579	571.0884	569.0827
3 h	1067.6749	1259.7312	1246.4008
5 h	1577.8662	1833.314	1809.2758
7 h	2021.3978	2310.6098	2280.5383
Time	**The Tube with 11 fins**		
	Re=1000	**Re=1500**	**Re=2000**
1 h	551.2066	613.6911	628.5596
3 h	1211.3304	1324.6057	1359.672
5 h	1753.1456	1897.1291	1953.8
7 h	2211.2828	2384.5758	2449.4652
Time	**The Tube with 15 fins**		
	Re=1000	**Re=1500**	**Re=2000**
1 h	556.2254	548.3738	-
3 h	1218.6818	1214.1003	-
5 h	1752.1832	1751.9004	-
7 h	2208.6264	2226.9176	-
Time	**Finless Tube**		
	Re=1000	**Re=1500**	**Re=2000**
1 h	477.1801	520.6518	539.1709
3 h	1069.4347	1153.6989	1201.4706
5 h	1553.3472	1689.7218	1735.9589
7 h	1973.8844	2138.2263	2199.004

Table A.2 Discharged cold energy values during melting for different types of tubes

DISCHARGED COLD ENERGY DURING MELTING (kJ)					
The Tube with 7 fins (small diameter)					
Time	**Re=1000**	**Time**	**Re=1500**	**Time**	**Re=2000**
1 h	448.3041	1 h	493.7468	1 h	459.017
2 h	1015.9644	2 h	1007.0009	2 h	931.6497
3 h	1402.8351	3 h	1416.0396	3 h	1365.8275
3 h10 min	1493.2719	3 h 25 min	1606.5708	3 h 45 min	1716.06
The Tube with 7 fins (big diameter)					
Time	**Re=1000**	**Time**	**Re=1500**	**Time**	**Re=2000**
1 h	504.3091	1 h	576.2106	1 h	585.469
2 h	869.5788	2 h	907.9708	2 h	946.4639
3 h	1146.7751	3 h	1306.6439	3 h	1302.7738
3 h50 min	1441.2511	3 h 35 min	1576.2119	3 h 45 min	1638.1376
The Tube with 11 fins					
Time	**Re=1000**	**Time**	**Re=1500**	**Time**	**Re=2000**
1 h	555.2559	1 h	632.7589	1 h	633.3763
2 h	894.0558	2 h	1041.1548	2 h	1337.935
3 h	1220.3964	3 h	1550.1354	3 h	1966.8821
3 h55 min	1576.7178	3 h 55 min	2065.9477	3 h 20 min	2039.5786
The Tube with 15 fins					
Time	**Re=1000**	**Time**	**Re=1500**	**Time**	**Re=2000**
1 h	636.2979	1 h	-	1 h	-
2 h	1020.5167	2 h	-	2 h	-
2 h55 min	1381.8937	3 h	-	3 h	-
Finless Tube					
Time	**Re=1000**	**Time**	**Re=1500**	**Time**	**Re=2000**
1 h	375.8135	1 h	400.5101	1 h	469.5189
2 h	846.2338	2 h	1022.5844	2 h	1150.4138
3 h	1125.3109	3 h	1503.8376	3 h	1612.1037
4 h	1478.1333	3 h 25 min	1638.3692	3 h 20 min	1714.9487